

**МІНІСТЕРСТВО ОСВІТИ І НАУКИ УКРАЇНИ
НАЦІОНАЛЬНИЙ АВІАЦІЙНИЙ УНІВЕРСИТЕТ
КАФЕДРА КОНСТРУКЦІЇ ЛІТАЛЬНИХ АПАРАТІВ**

ДОПУСТИТИ ДО ЗАХИСТУ
Завідувач кафедри, д.т.н, проф.
_____ **Сергій ІГНАТОВИЧ**

«__» _____ 2021р.

**ДИПЛОМНА РОБОТА
ВИПУСКНИКА ОСВІТНЬОГО СТУПЕНЯ «МАГІСТР»
ЗІ СПЕЦІАЛЬНОСТІ
«АВІАЦІЙНА ТА РАКЕТНО-КОСМІЧНА ТЕХНІКА»**

**Тема: «Покращення ресурсних характеристик літака шляхом оптимізації
заклепкових з'єднань»**

Виконавець: _____ **Хунсун ВАН**

Керівник: д.т.н., професор _____ **Михайло КАРУСКЕВИЧ**

Охорона праці: к.т.н., доцент _____ **Вікторія КОВАЛЕНКО**

Охорона навколишнього середовища:
д.т.н., професор _____ **Тамара ДУДАР**

Нормоконтролер: к.т.н., доцент _____ **Сергій ХИЖНЯК**

Київ 2021

**MINISTRY OF EDUCATION AND SCIENCE OF UKRAINE
NATIONAL AVIATION UNIVERSITY
DEPARTMENT OF AIRCRAFT DESIGN**

PERMISSION TO DEFEND

Head of the Department
Dr. of Sc., professor
_____Sergiy IGNATOVYCH
«___» _____ 2021

**MASTER DEGREE THESIS
ON SPECIALITY
"AVIATION AND ROCKET-SPACE ENGINEERING"**

Topic: « Improvement of the aircraft fatigue characteristics by the optimization of riveted joints »

Fulfilled by: _____ **Hongsong WANG**

Supervisor:
Dr. of Sc., professor _____ **Mykhailo KARUSKEVYCH**

Labor protection advisor:
Ph.D., associate professor _____ **Victoria KOVALENKO**

Environmental protection adviser:
Dr. of Sc., professor _____ **Tamara DUDAR**

Standards Inspector _____ **Sergiy KHIZHNYAK**

Kyiv 2021

НАЦІОНАЛЬНИЙ АВІАЦІЙНИЙ УНІВЕРСИТЕТ

Факультет аерокосмічний

Кафедра конструкції літальних апаратів

Освітній ступінь «Магістр»

Спеціальність 134 «Авіаційна та ракетно-космічна техніка»

Освітньо-професійна програма «Обладнання повітряних суден»

ЗАТВЕРДЖУЮ

Завідувач кафедри, д.т.н., професор

_____ Сергій ІГНАТОВИЧ

«___» _____ 2021 р.

ЗАВДАННЯ

на виконання дипломної роботи студента

ВАН ХУНСУН

1. Тема роботи «Покращення ресурсних характеристик літака шляхом оптимізації **заклепкових з'єднань**», затверджена наказом ректора від 08 жовтня 2021 року №2173/ст.
2. Термін виконання проекту: з 11.10. 2021р. по 20.12 2021 р.
3. Вихідні дані до проекту: опис проблеми вторинного вигину, опис типових заклепкових з'єднань.
4. Зміст пояснювальної записки: аналіз проблеми забезпечення ресурсу заклепкових з'єднань, застосування методу скінченних елементів для аналізу пружно-деформованого стану, розробка рекомендацій по зменшенню вторинного вигину заклепкових з'єднань.
5. Перелік обов'язкового графічного (ілюстративного) матеріалу: презентація PowerPoint з результатами дослідження.

6. Календарний план-графік

№ пор.	Завдання	Термін Виконання	Відмітка про виконання
1	Аналіз стану проблеми вторинного вигину заклепкових з'єднань	8.10.2021–12.10.2021	
2	Розробка методології розрахунку напружень в заклепкових з'єднаннях	13.10.2021–16.10.2021	
3	Проведення розрахунків	17.10.2021 22.10.2021	–
4	Розробка рекомендацій по застосуванню отриманих результатів	16.11.2021 30.11.2021	–
5	Виконання задач розділу «Охорона праці»	30.11.2021- 7.12.2021	
6	Виконання задач розділу «Охорона навколишнього середовища»	7.12.2021- 15.12.2021	
7	Редагування, підготовка презентації	15.12.2021-20.12.2021	

7. Консультанти з окремих розділів

Розділ	Консультанти	Дата, підпис	
		Завдання Видав	Завдання Прийняв
Охорона праці	к. біол. н., доцент Вікторія КОВАЛЕНКО		
Охорона навколишнього середовища	д. т. н, професор Тамара ДУДАР		:-

Дата видачі завдання: 11.10. 2021 р.

Керівник дипломної роботи _____

Михайло КАРУСКЕВИЧ

Завдання прийняв до виконання _____

Хунсун ВАН

NATIONAL AVIATION UNIVERSITY

Aerospace faculty

Department of aircraft design

Educational Degree "Master"

Specialty 134 «Aviation and Rocket – Space Engineering»

Educational Professional Program «Aircraft equipment»

APPROVED BY

Head of department

Dr. of Sc., professor

_____ Sergiy IGNATOVYCH

«___» _____ 2021

TASK

For the master degree thesis

HONGSONG WANG

1. Topic: «Improvement of the aircraft fatigue characteristics by the optimization of riveted joints», approved by the Rector's order №2173/CT. 8 October 2021.
2. Period of work: 11.10. 2021p. - 20.12.2021
3. Initial data: description of the secondary bending problem, description of the typical riveted joint.
4. Content: Analysis of the problem, application of finite elements method for the stress-strain analysis, development of the recommendation for secondary bending reduction.
5. Required material: Text of the Master's Thesis, PowerPoint presentation of the research results.

6. Thesis schedule:

№	Task	Time limits	Done
1	Analysis of the secondary bending problem	8.10.2021–12.10.2021	
2	Development of the methodology of riveted joints stress-strain analysis	13.10.2021–16.10.2021	
3	Calculations	17.10.2021–22.10.2021	
4	Recommendation development on the application of research results	16.11.2021–30.11.2021	
5	“Labor protection” tasks	30.11.2021- 7.12.2021	
6	“Environment protection” tasks	7.12.2021- 15.12.2021	
7	Explanatory note final revision	15.12.2021-20.12.2021	

7. Special chapter advisers

Chapter	Consultants	Date, signature	
		Task Issued	Task Received
Labor protection	PhD, associate professor Victoria KOVALENKO		
Environmental protection	Dr. of Sc., professor Tamara DUDAR		

8. Date of the issue of the task: 11 October 2021.

Supervisor _____
Student _____

Mykhailo KARUSKEVYCH
Hongsong WANG

РЕФЕРАТ

Пояснювальна записка дипломної роботи магістра «Покращення ресурсних характеристик літака шляхом оптимізації заклепкових з'єднань»:

89 с., 78 рис., 2 табл., 19 джерел

Дана дипломна робота присвячена оптимізації заклепкових авіаційних з'єднань шляхом зменшення вторинного вигину елементів обшивки літака при дії експлуатаційних навантажень.

В роботі було використано методи комп'ютерного проектування за допомогою CAD/CAE систем проектування та розрахунку, зокрема CATIA та ABAQUS.

Практичне значення результату дипломної роботи магістра полягає в підвищенні надійності та довговічності авіаційних конструкцій, за рахунок оптимізації геометрії заклепкових з'єднань.

Матеріали дипломної роботи магістра можуть бути використані в навчальному процесі та в практичній діяльності конструкторів спеціалізованих проектних установ.

Дипломна робота, заклепкові з'єднання, вторинний вигин, розрахунок напружено-деформованого стану, оптимізація геометрії

ABSTRACT

Master degree thesis "Improvement of the aircraft fatigue characteristics by the optimization of riveted joints"

89 pages, 78 figures, 2 tables, 19 references

This master thesis is dedicated to optimization of aviation riveted joints by the reduction of secondary bending of aircraft skin components under the action of operational loads/

The methods of computer aided design CAD/CAE have been used, particularly CATIA та ABAQUS.

The practical value of the diploma work lays in the improvement of the reliability and extension of the lifespan of aviation constructions by the optimization of the riveted joints geometry.

The materials of the master's diploma can be used in the aviation industry and in the educational process of aviation specialties.

Master's thesis, riveted joints, secondary bending, stress-strain analysis, geometry optimization

CONTENT

PART 1. SECONDARY BENDING ROLE IN AIRCRAFT FATIGUE.

STATE OF THE ART	(Number of page)
1.1 Research Background	
1.2 Research status	
1.3 Types of rivets	
1.3.1 Solid rivets	
1.3.2 Blind rivet	
1.3.3 Blind bolts	
1.3.4 Threaded Pin	
1.3.5 Swaged Pin	
1.4 Types of riveting	
1.4.1 Stamping riveting	
1.4.2 Rolling riveting	
1.4.3 Huck riveting	
1.4.4 Zinc alloy rivet rotation method	
1.4.5 Self-piercing riveting of solid rivets	
1.4.6 Semi-tubular rivet self-piercing riveting	
1.5 Metal fatigue	
1.5.1 The definition and characteristics of fatigue	
1.5.2 Classification of fatigue	
1.6 The importance of the secondary bending problem for new constructional materials	
1.6.1 The composite material bolt connection	
1.6.2 Technological measures to weaken the secondary bending effect	
Conclusion to Part 1	
PART 2. METHODOLOGY	
2.1 Improvement of aircraft fatigue	
2.2 Introduction of software used in simulation	

2.3 Introduction to the experimental group structure. Parameters	
2.3.1 Structural	
2.3.2 Material	
2.3.3 Loading	
2.4 Variables: Control groups.....	
2.4.1 Control group 1. Rivet diameter	
2.4.2 Control group 2. Staggered thickness	
2.4.3. Control group 3. Plate thickness	
2.4.4 Control group 4. Distance between rivets	
2.4.5 Control group 5. Single strap joint	
2.4.6 Control group 6. Double strap joint	
2.5 General approach for the evaluation of secondary bending	
Conclusion to Part 2	
PART 3. SECONDARY BENDING FE ANALYSIS AND	
RECOMMENDATIONS FOR RIVET JOINTS IMPROVEMENT	
3.1 Finite Element Analysis Result of experimental group	
3.2 Finite Element Analysis Results of control groups	
3.2.1 Result of control group 1	
3.2.2 Result of control group 2	
3.2.3 Result of control group 3	
3.2.4 Result of control group 4	
3.2.5 Result of control group 5	
3.2.6 Result of control group 6	
3.3 Calculation of bending factor	
3.4 Result analysis	
3.5 Recommendations for rivet joints improvement	
3.5.1 Increase the size of the Rivet	
3.5.2 Set the lap joint with a staggered sheet thickness	
3.5.3 Increase plate thickness	
3.5.4 Increase the distance between the rivets	

3.5.5 Design a symmetrical and non-eccentric structure	
Conclusion to Part 3	
PART 4. ENVIRONMENTAL PROTECTION	
4.1 Requirements towards aircraft safety in terms of its construction in China	
4.2 The impact of aviation manufacturing on the environment	
4.3 Methods how to protect the environment from this impact	
Conclusion to Part 4	
PART 5. LABOR PROTECTION	
5.1 Introduction	
5.2 Analysis of working conditions in the workplace	
5.2.1 Workplace organization	
5.2.2 List of harmful and dangerous production factors	
5.2.3 Analysis of harmful and dangerous production factors	
5.2.3.1 Microclimate in the work area	
5.2.3.2 Non-ionizing electromagnetic fields and radiation	
5.2.3.3 Produce noise, ultrasonic, infrasound	
5.2.3.4 Static electricity	
5.3 Labor protection measures	
5.4 Fire safety at the production site	
Conclusion to Part 5	
GENERAL CONCLUSIONS	
REFERENCES	

ABBREVIATIONS

ICAO – International Civil Aviation Organization;

EASA – European Union Aviation Safety Agency;

FAA – Federal Aviation Administration;

FAR – Federal Aviation Regulations;

MP – Mechanical properties;

MC – Mechanical characteristics;

FE – Finite Element

SB – Secondary bending

NL – Neutral line

INTRODUCTION

The present master's work is devoted to the problem of the aircraft fatigue enhancement by the improvement of structural joints design. Because the riveting process is easy to check, easy to repeat assembly and replacement, and easy to repair, it has become one of the main methods for fixing the thin plates, longitudinal beams and strengthening fixtures of the aircraft fuselage.

It's known that riveted joints produced by the laps, cause the problem which is called secondary bending. Due to the eccentricity of the geometric shape of the parts, the structural parts under pressure are bent. The eccentricity mentioned here will cause out-of-plane displacement, and the generation of out-of-plane displacement will cause additional bending. This kind of bending which is not caused by the applied bending moment, is called secondary bending.

The secondary bending will generate additional stress in the components of aircraft riveted joints. By the reduction of the secondary bending, the fatigue life of the component can be extended.

The aim of the work is to reduce the influence of secondary bending on the fatigue characteristics of the aircraft by changing the structure of the riveted joints. To gain this aim, the following **objectives** should be solved:

1. To analyze design of the riveted joints of contemporary aircraft.
2. To select typical riveted joint for further stress-strain analysis.
3. To develop procedure of the finite element analysis for the selected component.
4. To analyze stress-strain state in the selected components by the FEA under the action of loads close to operational.
5. To analyze influence of the riveted joint geometry on the magnitude of the secondary bending.
6. To develop recommendation on the practical application of the Master work results.

In the process of the work, the international airworthiness requirements and standards have been taking into account: 33 97-NM-184-AD Fuselage Longitudinal Lap Joints and Circumferential Joints; 90 93-NM-62-AD Inspect Rivet Heads; 460 FAA-2005-23196 Lap joints of the fuselage skin; 462 93-NM-125-AD Universal Joint Assemblies; 801 91-NM-57-AD Fuselage Rivets; 3703 93-NM-139-AD Lap Joints; 3746 93-NM-36-AD Rivet Heads; 9768 FAA-2006-24697 Rivet inspection; 11964 98-NM-319-AD Fuselage Skin Lap Joints; 12188 90-NM-291-AD Lap Joint Rivets.

The actuality of the work is proved by the requirements to the aircraft fatigue as well as by the numerous papers in the selected field. The papers of Schijve, J. “Fatigue of structures and secondary bending in structural elements”, Skorupa, M. “Observations and analyses of secondary bending for riveted lap joints”, Skorupa, «Modelling the secondary bending in riveted joints with eccentricities», Chaves, «Analysis of fastened joints – part 1 : the influence of secondary bending», Rijck, J & Fawaz, «A Simplified Approach for Stress Analysis of Mechanically Fastened Joints», Zhao, Libin & Xin «Secondary bending effects in progressively damaged single-lap, single-bolt composite joints», de Rijck, «Stress analyses of mechanically fastened joints in aircraft fuselages», Machniewicz, «Numerical and experimental investigation of the secondary bending of riveted lap joints», should be mentioned here.

The guide for the Master work issued by the aircraft design department was used in all stages of the work on the diploma work.

PART 1. SECONDARY BENDING ROLE IN AIRCRAFT FATIGUE.

STATE OF THE ART

1.1 Research Background

Riveted joints are widely used in aviation, aerospace, machinery, mining, automobiles and ships due to their good mechanical properties, low cost, and strong applicability to the environment. In aircraft manufacturing, riveted connections are particularly widely used. According to rough estimates, there are about 1.5 to 2 million rivets and bolts on a large aircraft. With the rapid development of the aviation industry, the aircraft is moving towards higher speed and larger size, the working environment is getting worse and worse, the structural load is increased, and the stress state is complex. In recent years, there have been a series of global aircraft accidents, and aircraft accidents caused by stress concentration caused by riveting have also occurred from time to time. According to statistics, aircraft strength problems occur during use.

More than 80% of aircraft accidents is caused by fatigue damage, on the fuselage or wing frame, so single lap is inevitable; the load path of single lap is eccentric, resulting in additional bending and deformation of the skin surface, which is generally called the second bending. One of the most important assembly techniques in aircraft structures is the use of bolts and rivets to connect. Bolted connections are easy to disassemble to facilitate repair and replacement of damaged parts; rivets are more stable and safer, and both are single-pass connections. This places further demands on the technology used to assemble structural components.

A large number of studies have been done on the secondary bending of single-lap connecting members at home and abroad; the literature has confirmed that secondary bending exists in a large number of aircraft structures, and they measured 150 positions.

Measure the strain of different structures and found that 86% of the components have different degrees of secondary bending exist. Secondary bending affects

various macroscopic failure modes, in this situation, the mode of failure and final load will be changed dramatically.

1.3 Research status

For the measurement of secondary bending, researchers have adopted different methods to accurately measure the out-of-plane displacement of the composite bolted joint in the experiment. For example, Starikow R and Ireman T [1] affixed strain gauges between two rows of bolts to measure the strain distribution, thereby measuring the degree of bending at a certain point to measure the secondary bending effect of the structure (Fig.1.1).

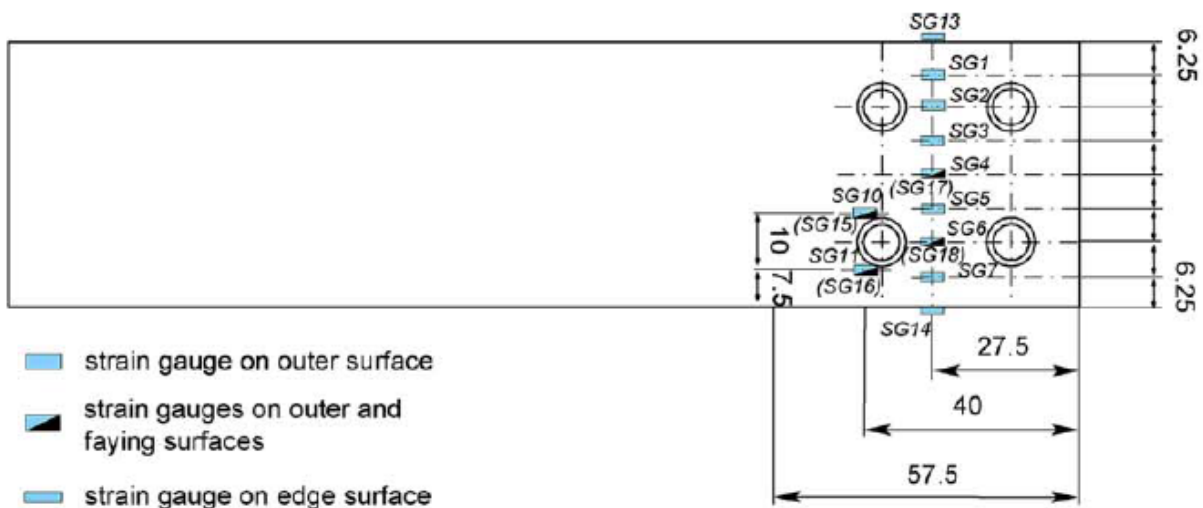


Fig.1.1 - Measurement the strain distribution [1]

Johan Ekh [2] used an optical measurement system to measure the lateral displacement of the free edge parallel to the loading direction of the structural lap area under the tensile load, and combined the finite element method to output the displacement of the specimen in three directions. Through parametric research, the deformation of the specimen under 10 different conditions (with only one parameter changed in each case) was discussed and analyzed, and it was found that the double-nail composite material-aluminum plate bolt connection will aggravate the secondary bending when the overlap area is reduced. When the thickness of the

aluminum plate is reduced, the secondary bending phenomenon will be weakened (Fig.1.2).

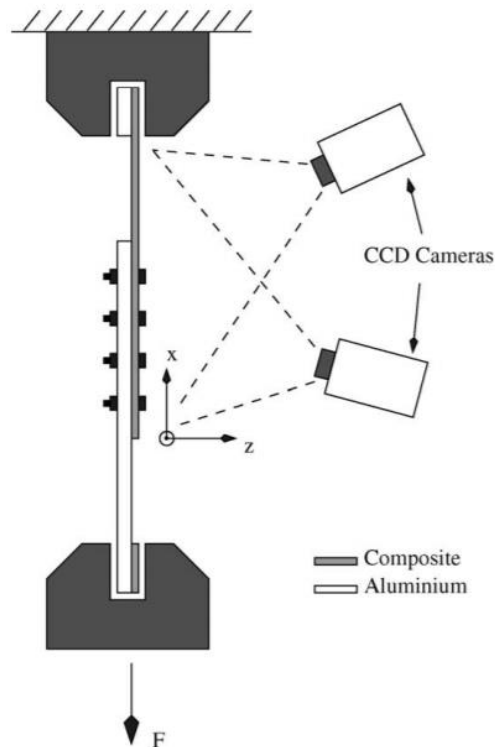


Fig.1.2 - Schematic of experimental set-up [2]

M. Skorupa [3] studied the secondary bending phenomenon of the rivet lap structure through experiments and numerical analysis. The experiment used strain gauges to measure the stress caused by secondary bending, and discussed several variables related to the geometric parameters of the joint. The effect of secondary bending on the fatigue life of rivet lap joints. It is found through research that the maximum moment generated by the secondary bending occurs on the eccentric load transmission path, that is, the rivet row. For the connection of more than two rivets, the maximum bending moment always occurs on the outermost side. The plane deformation caused by the second bending is the largest (Fig.1.3).

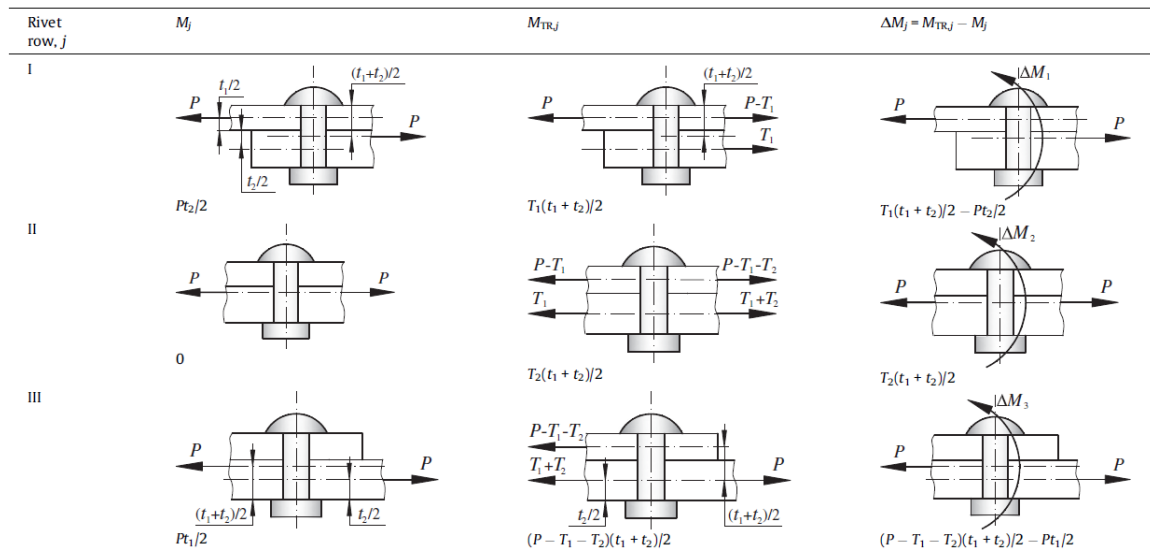


Fig.1.3 - Bending moments on the rivet rows for a three-row lap joint.

J. Schijve [4] proposed to use the neutral line model method to predict the maximum bending deformation of the structure, that is, the magnitude of the change in the secondary bending. This method can calculate the secondary bending at any position of the connecting structure by calculating the centerline deformation of a simple lap joint. bending. According to the calculation results of the model, the size of the secondary bending decreases significantly with the decrease of the plate thickness, and the increase of the spacing between the rivet rows will weaken the secondary bending effect of the structure. In addition, Schijve's research found that reducing the secondary bending effect of the outer ring fastener hole will weaken the stress at this position, which can be achieved by the thickness of the staggered plate in the overlapping area (Fig.1.4, 1.5).

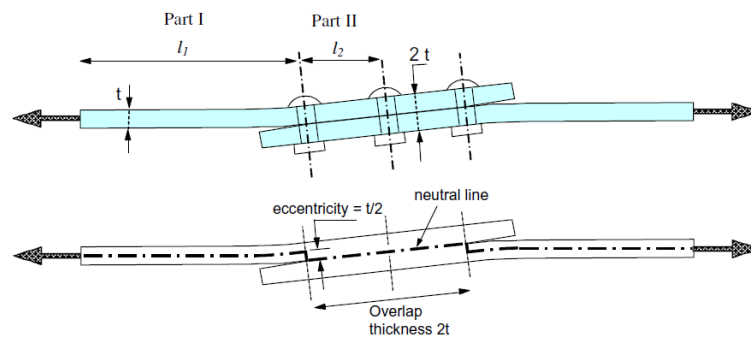


Fig.1.4 - Secondary bending in a riveted lap joint under tensile loading due to eccentricities in the neutral line [4]

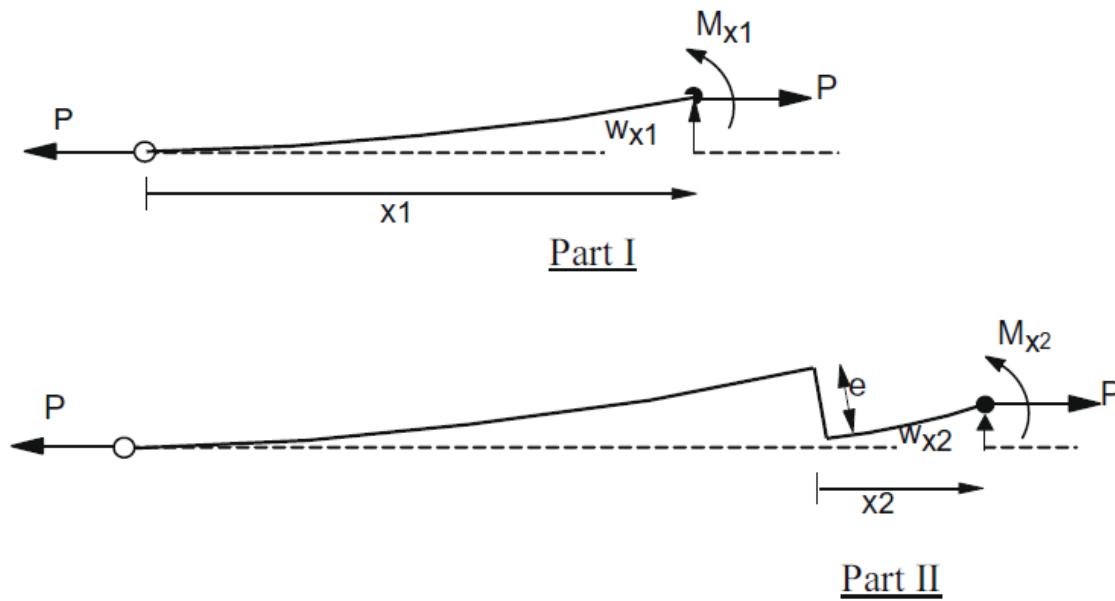


Fig.1.5 - Two parts of the neutral line model in Fig.1.4

Joakim Schom [5] studied the influence of the length of the lap area on the secondary bending effect of the structure, and concluded that the secondary bending will affect the macroscopic failure mode of the structure and affect the maximum load-bearing capacity. It also points out that under tension, the second bending will increase the contact area between the fastener and the hole, which will reduce the extrusion stress and increase the extrusion strength. At the same time, it is also studied that under compressive load, the compressive strength decreases due to the existence of secondary bending (Fig.1.6).

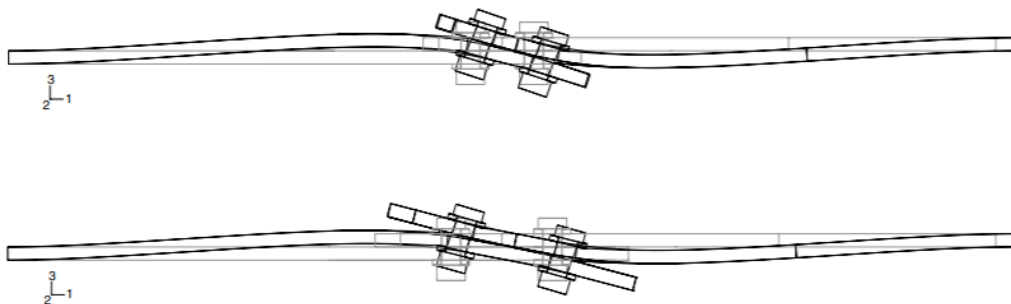


Fig.1.6 - Lateral deflections at tensile loading for joints with 20 and 32mm row spacing. Displacements are magnified

1.3 Types of rivets

1.3.1 Solid rivets

Solid rivets are the oldest and highly reliable fastener types according to records. Solid rivets play a very important and indispensable role in reliability, including safety. A solid rivet is composed of a shaft and a head, and the deformation operation is realized by a hammer or a rivet gun. In the experimental operation, we need to choose a solid rivet with a suitable head. Round, countersunk, flat, button, regular, oval, trust, and disc are the common head styles of solid rivets. (Fig.1.7).

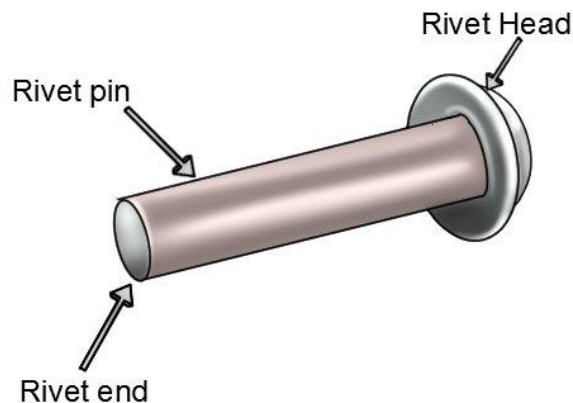


Fig.1.7 - Solid rivet

1.3.2 Blind rivet

Blind rivets are a type of rivets. They are used for applications where access to the back side (blind side) of the component to be connected is limited or inaccessible. Its specific structure roughly consists of two parts. The first part is called the rivet body while the second part is called the mandrel. It is cost-effective, durable, and lighter than bolts/screws, but it is difficult to remove after placement, protruding from the sheet metal surface, which may cause danger and reduce aerodynamic performance (Fig.1.8).

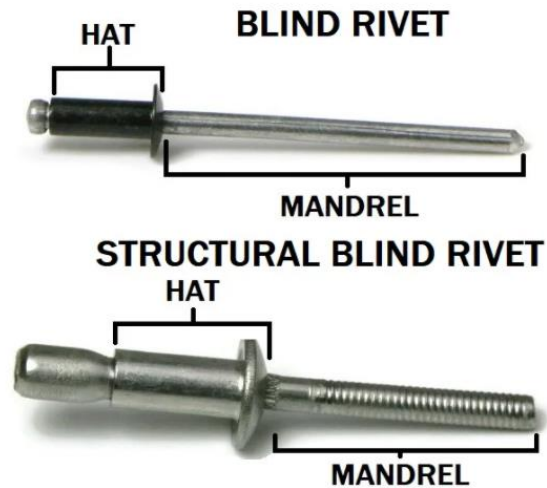


Fig.1.8 - Blind rivet

1.3.3 Blind bolts

Blind bolts are structural fasteners that have higher strength and adaptability than typical rivets or welds. They were developed to establish a strong connection when traditional rivets or hexagonal bolts are difficult to install or cannot complete the work (Fig.1.9).



Fig.1.9 - Blind bolts

1.3.4 Threaded Pin

When two parts are to be assembled to support a load, the fasteners commonly used are defined as threaded pins. The size of the thread and the mechanical properties of the fastener material will determine the strength capability. (Fig.10).



Fig.10 - Threaded Pin

1.3.5 Swaged Pin

It is called a compression rivet, which means that the Collar on the rivet is forcibly squeezed into the groove of the PIN to achieve the riveting requirement during the riveting process (Fig.1.11).



Fig.1.11 - Swaged Pin

1.4 Types of riveting

1.4.1 Stamping riveting

The traditional riveting technology that emerged and studied earlier. Manual hammering and machine punching apply riveting force (mostly impact force) to the axial direction. Disadvantages: If the riveting force required for riveting is large, it is difficult to riveting rivets with larger diameters.

1.4.2 Rolling riveting

During the rolling and riveting process, the riveting punch (rivet rod) is at a sharp angle with the rivet axis, and it also has a downward pressing movement when doing a specific movement track, so that the rivet head is subjected to continuous partial and even rolling action to form a need to be riveted shape. It can be divided into radial type and pendulum type. Compared with traditional rivet riveting, rolling riveting has no relative sliding and impact during the riveting process, high riveting quality, low energy consumption (small riveting force, high efficiency), low noise and vibration, and can riveting a variety of materials. It has a wide range of applications, which can be used for riveting with rivets and riveting without rivets, and it is competent for many difficult-to-rive materials and special joint shapes. Just change the shape of the riveting punch according to the required riveting.

1.4.3 Huck riveting

Using the principle of Hooke's law, after clamping the joint with special equipment for pulling rivets, the metal of the collar is squeezed and filled into the groove of the stud with multiple annular grooves to make the collar and the stud tight a combination of fastening methods. Advantages: high clamping force, good vibration and fatigue resistance, and high work efficiency. Disadvantages: rivets are longer and heavier, and the manufacturing difficulty and price are more expensive than traditional rivets. It is mainly suitable for industries with high added value and high load requirements. Huck fasteners are currently the only fasteners in the world that do not require torsion to generate fastening force. The tightening force depends

on the diameter of the screw and the matching collar. There are more applications for heavy-duty trucks.

1.4.4 Zinc alloy rivet rotation method

Using the principle of low melting point of the rivet material and frictional heat generation, the rivets rub against each other when they are rotated and drilled into the sheet, so that the material is locally heated and softened, and plasticity is increased to form a pier, so as to achieve the purpose of riveting. Advantages: No need to drill before riveting, relatively simple process and convenient operation. The riveted products are beautiful, with low labor intensity and high production efficiency. Disadvantages: Rivets are expensive to manufacture, and cooling factors must be considered during the riveting process.

1.4.5 Self-piercing riveting of solid rivets

It is to fix the sheet to be connected between the die and the blank holder, and the solid rivet penetrates the upper and lower sheets through the downward movement of the punch, and punches out a small piece of metal, and then under the reaction force of the lower mold. The part of the lower sheet material is pressed into the annular groove to form an interlocking mechanism. The self-piercing riveting of solid rivets is a typical process of large local plastic deformation, including two processes of punching, cutting and extrusion. Advantages: low cost and high connection quality. Disadvantages: riveting noise is large, rivet geometry, blank holder force, gap between rivet and die (lower die) have a greater impact on riveting quality.

1.4.6 Semi-tubular rivet self-piercing riveting

When the semi-hollow rivet is pressed down by the punch, the rivet penetrates the upper sheet, and under the combined action of the die and the punch, the tail of the rivet opens in the lower metal, forming a mechanical interlocking mechanism between the two sheets. Note that for the self-piercing riveting process of semi-

tubular rivets, when riveting two layers of the same metal material, put the thicker one on the lower layer; when riveting two layers of different metal materials, put the material with good plasticity on the lower layer; when riveting metal and non-metal materials, Put the metal material on the lower layer. Advantages: It can connect multiple layers of materials, does not require pre-drilling, is fatigue-resistant, has little impact on the environment, and is convenient for quality inspection. Compared with solid rivet self-piercing riveting, it has no sparks, no waste, low energy consumption and low noise. Disadvantages: high precision of mold manufacturing, matching of rivet and sheet material properties.

1.5. Metal fatigue

1.5.1 The definition and characteristics of fatigue

The International Standards Organization defines fatigue in the "General Principles of Metal Fatigue Test": the change in the performance of metal materials under repeated stress or strain is called fatigue.

Fatigue damage has the following characteristics:

1. Low stress: The load caused by fatigue failure is often much smaller than the tensile strength σ_b or even the yield stress σ_s of the material or structure.
2. Sensitivity: The load value corresponding to the occurrence of fatigue failure is not only related to the material itself, but also related to the surface condition, use environment and the shape of the part.
3. Suddenness: Fatigue fracture is mostly manifested as brittle sudden fracture without obvious plastic deformation, and the occurrence of fatigue failure has a certain degree of unpredictability.
4. Timeliness: Fatigue failure is the result of repeated action of cyclic loads. It takes a certain period of time to occur, and the time of occurrence of fatigue is also one of the important indicators to measure the fatigue performance of materials or structures.

5. Fatigue fracture: On the macroscopic fracture, fatigue damage has obvious fatigue source area, crack propagation area and final fracture area, which is different from other fracture fractures.

1.5.1 Classification of fatigue

Fatigue process is classified according to the different parameters of the loading and nature of the damage:

1. According to the strain. Low cycle fatigue: Refers to fatigue with high stress and low life (cycles less than $10^2 \sim 10^5$), also known as plastic fatigue or strain fatigue.

High cycle fatigue: Refers to fatigue with low stress and high life (the number of cycles is generally greater than 10^5), and is the most common type of fatigue.

2. According to load type. Random fatigue: Fatigue whose frequency and stress amplitude change over time

Contact fatigue: Fatigue that refers to the occurrence of pitting, surface layer cracking or peeling on the contact surface of the part under the action of the contact pressure cycle, resulting in the failure of the part

Fretting fatigue: When the surfaces of two parts meet, under the condition of a small range of reciprocating relative motion, the fatigue on the contact surface usually has three stages of adhesion, oxidation, and fatigue, which are the result of a combination of mechanical and chemical processes.

Impact fatigue: Fatigue caused by multiple impacts

3. According to ambient temperature. Low temperature fatigue: The parts are fatigued under cyclic stress in an environment below room temperature

High temperature fatigue: Fatigue in a high-temperature environment. The high temperature here mostly refers to the temperature above the melting point of half of the metal. Fatigue and creep are the result of the combined effect of fatigue and creep during high-temperature fatigue.

Thermal fatigue: The cyclical change of strain caused by the cyclical change of temperature, and then the fatigue that causes the failure phenomenon.

4. Acoustic fatigue. Fatigue of structural parts caused by noise such as electromagnetic noise, aerodynamic noise or structural noise.

5. Corrosion fatigue. Fatigue caused by the combined action of corrosive media and cyclic load.

There are many factors influencing fatigue:

1. The effect of stress concentration. The stress concentration is the main part of fatigue failure. Under normal circumstances, when the nominal stress is still less than the yield stress, the stress concentration part of the structural part has entered a plastic state, and the local stress and strain state determines the fatigue strength of the structural part. Therefore, the stress concentration has a greater impact on the fatigue life of the structural part.

2. Influence of load parameters. The load factors that affect fatigue strength mainly include load frequency, load type, average stress, load waveform, and intermediate stop and duration of load, etc.:

Influence of load types: Fatigue loads mainly include tension and compression, bending, and torsion. The same test piece may bear multiple loads in multiple directions at the same time. Different load types affect the stress distribution in the test piece, which in turn affects the fatigue strength of the test piece.

The influence of loading frequency: when the working frequency f is less than

At 1000 Hz, the fatigue limit of the material or structure will increase slightly as the frequency increases.

The effect of average stress: The study found that under the condition of equal stress amplitude, the fatigue life of symmetrical cyclic loading with an average stress of 0 is higher than that of the average stress.

Load stop and continuous influence: Tests show that load stop has a certain influence on fatigue life, but basically has no influence on fatigue limit value.

3. Influence of size. A large number of tests have shown that the fatigue strength of the sample decreases with the increase of the size. There are two main

reasons for the difference in the fatigue strength of the large and small test pieces: for the test pieces that are in the same uniform stress field, the large There are more fatigue damage sources in the size test piece than the small size test piece; for the test piece that is in the same non-uniform stress field, the stress in the fatigue damage zone of the large size test piece is more serious than that of the small size test piece.

4. Effect of surface condition. The outer surface of the test piece often has a higher stress level and more processing defects. Therefore, fatigue cracks mostly occur on the surface, and the treatment of the surface condition has a greater impact on the fatigue strength. The influence of surface state on fatigue strength mainly includes factors such as surface roughness, surface stress state, and surface structure.

1.6. The importance of the secondary bending problem for new constructional materials

1.6.1 The composite material bolt connection

Composite material bolted connections can be divided into single-shear connection and double-shear connection according to the different forces of the bolts. The single-shear bolt connection under the action of tensile force will generate a bending moment at the bolt due to the influence of eccentric load. The out-of-plane deformation of the joint is called "secondary bending". And because the interaction force between the two plates, the force between the bolt and the hole wall, and the hole edge stress distribution have a complicated mechanical response under the influence of secondary bending, this will cause the hole edge stress to be distributed in the thickness direction. Uneven, reducing joint strength.

Clamping method, laminate thickness, external load, laminate stiffness loss and other factors may affect the degree of secondary bending.

1.6.2 Technological measures to weaken the secondary bending effect

Change the clamping method: In the process of static load tensioning of the laminates, the clamping methods are divided into centering clamping and eccentric clamping. Both centered clamping and eccentric mounting sandwich plates have

different directions and different degrees of deviation, resulting in different degrees of bending; centering clamping has a greater impact on the secondary bending effect of laminates than eccentric clamping.

Control the thickness of the laminate: With the increase of the thickness of the laminate, the secondary bending effect of the laminate becomes serious. The entire laminate has such a manifestation, not only at the connection, but the increase in the thickness of the laminate can reduce the local bending stress of the laminate, but it will increase it. The secondary bending effect of the laminate; for this reason, the increase in the thickness of the laminate aggravates the bending stress, but the secondary bending effect at the joint is slowed down.

Adjust the size of the external load: With the increase of the external load, the secondary bending effect at the connection of the laminates is slowed down, but when the external load reaches a certain level, its impact on the secondary bending is weakened; in addition, the secondary bending effect at the connection also decreases with the increase in thickness. getting more serious. Under the same load, the secondary bending effect of the eccentric clamping is smaller than that of the center clamping; with the increase of external load, the secondary bending effect of the two clamping methods at the joint has the same degree of reduction; it also further proves the eccentricity In the case of clamping, the secondary bending effect at the joints of the laminates is smaller.

Monitoring laminate stiffness loss: The loss of laminate rigidity aggravates the degree of bending of the connecting piece, which intensifies the secondary bending effect of the laminate.

Conclusion to Part 1.

The first chapter deals with main tasks of the research with emphasize on aspects affecting secondary bending of riveted joints in aircraft structures. It is shown that the secondary bending is an important factor affecting aircraft structure fatigue. The works of contemporary scientists are discussed to prove the value of the

present Master's degree work. The design of riveted joints is described for the understanding of the appropriate methods for the structural integrity improvement.

The problem of the aircraft fatigue is described with indication of main factors influencing metal fatigue phenomenon.

As a result of first part the aim and objectives of the Master's work have been formulated. These are:

The aim of the work is to reduce the influence of secondary bending on the fatigue characteristics of the aircraft by changing the structure of the riveted joints.

To gain this aim, the following **objectives** should be solved:

1. To analyze design of the riveted joints of contemporary aircraft.
2. To select typical riveted joint for further stress-strain analysis.
3. To develop procedure of the finite element analysis for the selected component.
4. To analyze stress-strain state in the selected components by the FEA under the action of loads close to operational.
5. To analyze influence of the riveted joint geometry on the magnitude of the secondary bending.

PART 2. METHODOLOGY

2.1 Improvement of aircraft fatigue

Fatigue failure of metal structures is a well-known technical problem. As early as the 19th century, several serious fatigue failures have been reported. The application of a single load is far lower than the static strength of the structure and will not cause any damage to the structure. However, if the same load is repeated multiple times, it may cause a complete failure. Repeated load application can initiate the fatigue mechanism in the material, leading to the nucleation of small cracks, then crack growth, and finally complete failure. So far, the history of engineering structures has been marked by multiple fatigue failures in machinery, welded structures, and airplanes. Such failures lead to catastrophic accidents from time to time. But the economic impact of non-catastrophic fatigue failures is huge. Structural fatigue is now generally regarded as a serious problem.

Riveting is one of the main methods for bonding aircraft fuselage panels, strings, and hardeners together. Although alternative methods such as welding and bonding exist, this method will continue to be used in the foreseeable future. The main advantages of riveted joints include low production costs, the use of traditional metal working tools and techniques, the possibility of automation of the riveting process, the convenience of inspection, the possibility of repeated assembly and disassembly, and the good hole filling performance of rivets. Last but not least important, long-term experience in the industry with riveting joints. However, at the same time, riveted joints are a key element of fatigue in the metal fuselage structure. For riveted joints with eccentric load paths, the bending stress that occurs under nominal tensile loading of the joint must also be considered. The bending caused by the tensile load on the joint is called secondary bending. The eccentricity of the crack path is inherent to the riveted joints commonly found in aircraft fuselages, namely longitudinal knee joints and circumferential single-strap joints.

The calculation method of the second bending can be defined as:

$$k_b = \frac{S_b}{S} \quad (2.1)$$

Where S_b is the maximum nominal bending stress and S is the nominal tensile stress applied to the joint. Both S_b and S are calculated as the thick part of the table, that is, rivet holes are ignored.

The maximum bending moment occurs at the eccentricity, that is, the fastener row. For loop joints with more than two rivet rows, the position of the maximum bending moment is always located in the outer row. It is defined as:

$$S_{b,i} = \frac{6M_{b,i_{max}}}{Bt_i^2} \quad (2.2)$$

The subscript i represents the critical position, $M_{b, i_{max}}$ are the maximum bending moments, and B and t_i represent the total width and thickness of the specimen, respectively. (Fig. 2.1)

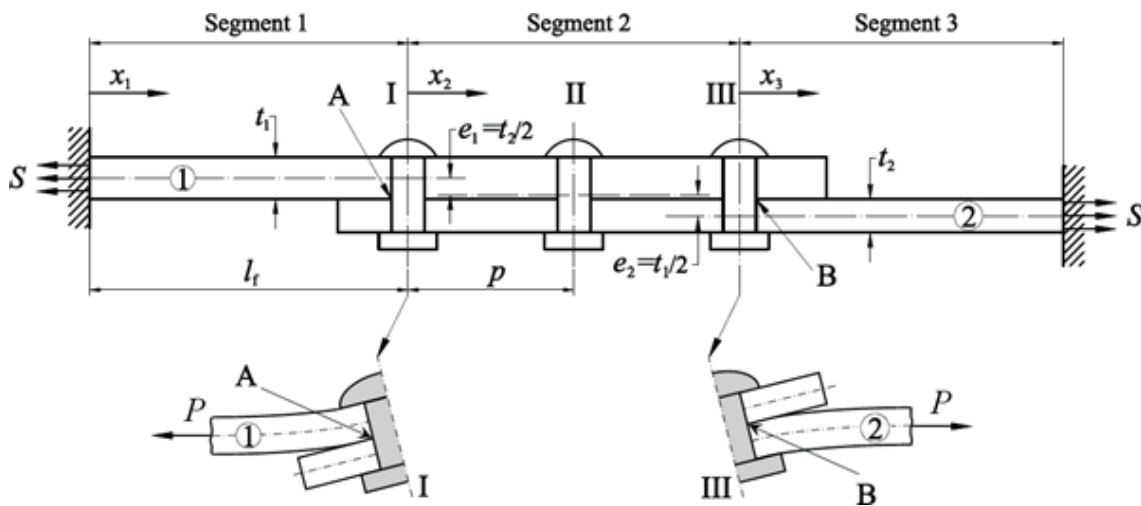


Fig.2.1 - Schematic diagram of riveting structure

The nominal stress due to the secondary bending can be equal to or even exceed the applied stress. The fracture study of riveted joints shows that the fatigue crack core appears at the position of maximum bending pressure

The subject of this article is to simulate the secondary bending of riveted joints with several different experimental control groups based on two simple theoretical concepts proposed in the literature. Through computer software simulation, the model is tested and numerically verified. Finally, the correlation between the secondary bending calculated using a simple model and the observed fatigue characteristics of the riveted specimen is studied, so as to find a way to reduce the effect of secondary bending on the fatigue of the aircraft.

2.2 Introduction of software used in simulation

Catia. Dassault Systems has developed a multi-platform 3D software suite called CATIA. It has several working modules, namely CAD, CAM and CAE. Dassault is a French advanced engineering software company whose business scope includes aviation and 3D design and digital modeling, as well as product life cycle management business. As a solid modeling tool, CATIA has both 3D parametric features and 2D tools. With the functions of these modules, it can be used to solve every process from design to manufacturing. While creating solid models and assemblies, functions such as orthogonal and cross-section, auxiliary and isometric or detailed 2D drawing views are also provided by CATIA.

The design and manufacture of aerospace parts are sufficiently complex that there is no need to worry about the structural integrity of the parts. This is where the use of composite materials can relieve some of the stress.

Compared with alternative metals, composite materials can produce lightweight, impact-resistant parts. This allows OEMs to produce higher quality parts, which is especially important for aircraft when we consider safety protocols.

A feature of composite materials called lightweight, has a beneficial effect on environmental protection. High fuel efficiency and low carbon emissions are achieved under the lighter weight of the aircraft. Under the background that the strategy of reducing carbon footprint has been widely adopted by original equipment manufacturers, a good solution is provided. CATIA has three advantages in the design and manufacturing of aerospace composite materials:

First: save time and money. CATIA V5 uses the automatic update function in the field of design change management functions to reduce the impact of changes on the design to manufacturing process. With the automatic update function, users do not need to restart the entire design process, so a lot of time and money will be saved.

Second: geometric configuration. The geometric configuration of composite parts makes the design of these parts quite complicated, which increases the risk of

errors in design accuracy. However, CATIA Composites Design 3 (CPD) supports the design of multiple composite material configurations. CATIA CPD 3 enables you to manage multiple part geometries, including core rebar parts, better than using standard composite design solutions.

Third: Productivity check. With CATIA, in-depth manufacturability checks enable users to predict the behavior of composite materials on complex surfaces. For example, users can predict manufacturing problems (such as wrinkles), and can take steps to correct any problems and generate flat patterns. This is important when trying to produce high-quality parts while reducing costs and avoiding wasted time.

CATIA's three major manufacturing advantages can help improve the production of aerospace parts, including: avoiding restarting the design process through automatic updates, saving money and time, and being able to manage multi-part geometries better than standard composite design solutions. Predict the behavior of composite materials on complex surfaces and make changes if necessary.

The graduation project will use Catia software to model the riveting structure of the aircraft skin. By changing the riveting structure, methods and feasibility studies to reduce the impact of secondary bending on the fatigue life of the aircraft will be studied.

Abaqus. Abaqus is used in the automotive, aerospace and industrial products industries. The product is welcomed by non-academic and engineering research institutions because of its extensive material modeling capabilities and program customization. For example, users can define their own material models so that new materials can be simulated in Abaqus. Abaqus also provides a good set of multi physics functions, such as coupled acoustic-structure, piezoelectric, and structure-porosity functions, making it attractive for production-level simulations that need to couple multiple fields. Abaqus was originally designed to solve nonlinear physical behavior; therefore, the package has a wide range of material models, such as elastic (rubber-like) and super-elastic (soft tissue) material functions.

As a finite element software, ABAQUS is extremely powerful. Using it, both simple linear analysis and complex nonlinear problems can be solved easily. A unit

library is built in ABAQUS. Almost any geometric shape can be simulated using this cell library. This software material model library is also very rich. It can simulate different problems in other engineering fields while solving structural problems. Here, phenomena such as heat conduction and mass diffusion, acoustic analysis and geomechanical analysis are included. At the same time, it can also simulate the performance of typical engineering materials.

In the design of this article, ABAQUS is used to perform finite element analysis on the riveted structure to obtain the stress distribution of the riveted structure, so as to analyze the effect of structural changes on the secondary bending.

2.3 Introduction to the experimental group structure. Parameters

2.3.1 Structural

In the first lap joint two sheets are connected by three rows of rivets. As discussed later, this is a experimental group.

Figure showed below (Fig.2.2) is the three views of the plate, as we can see from the figure, the length of the plate is 105mm, width is 24mm, and the thickness of the plate is 2mm. The three rivet holes are 5mm in diameter and 15mm apart.

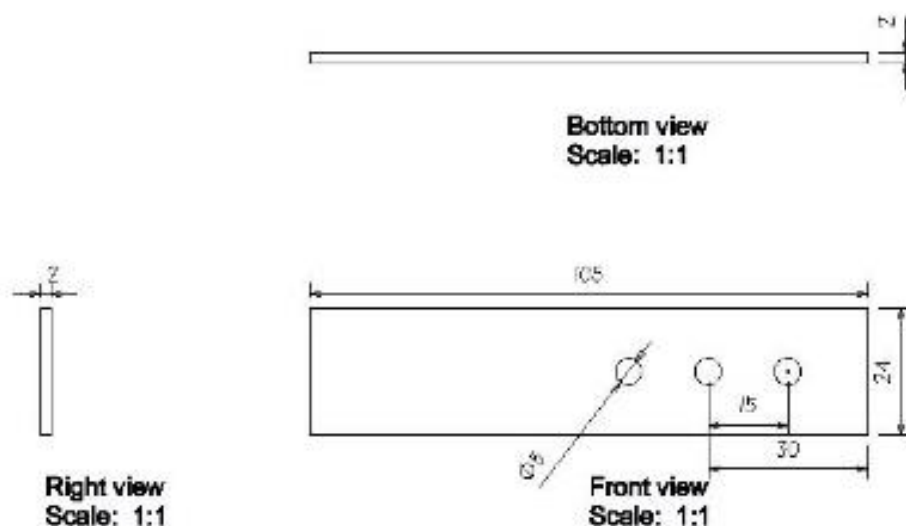


Fig. 2.2 - Experimental group structure

The figure below (Fig.2.3) shows a schematic diagram of riveting in an unloaded state.

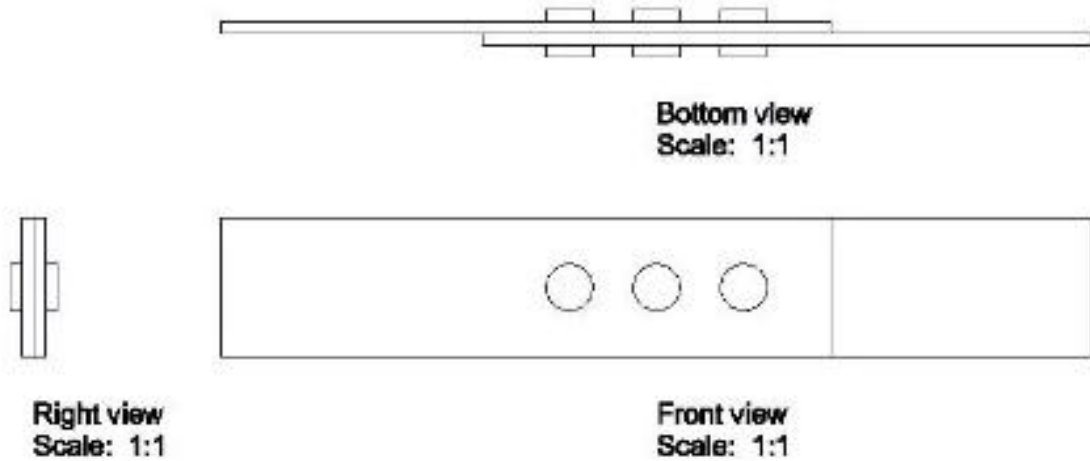


Fig. 2.3 - Schematic diagram of riveting in an unloaded state

2.3.2 Material

As shown in the figure below (Fig.2.4, Fig.2.5), set the rivet material as steel.

The mass density of it is 7.8×10^{-9} , and the Young's Modulus is 210000Mpa and the Poisson's Ratio is 0.3.

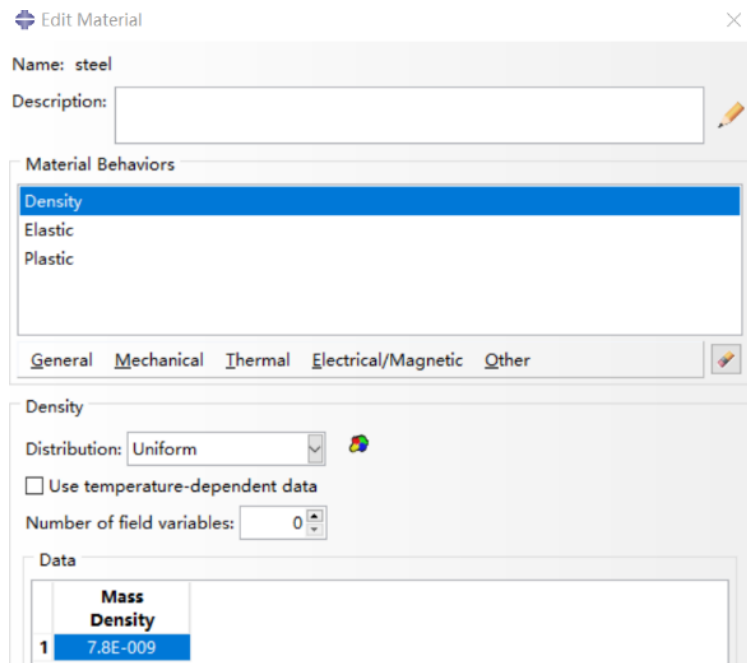


Fig. 2.4 - The material density setting of experiment group

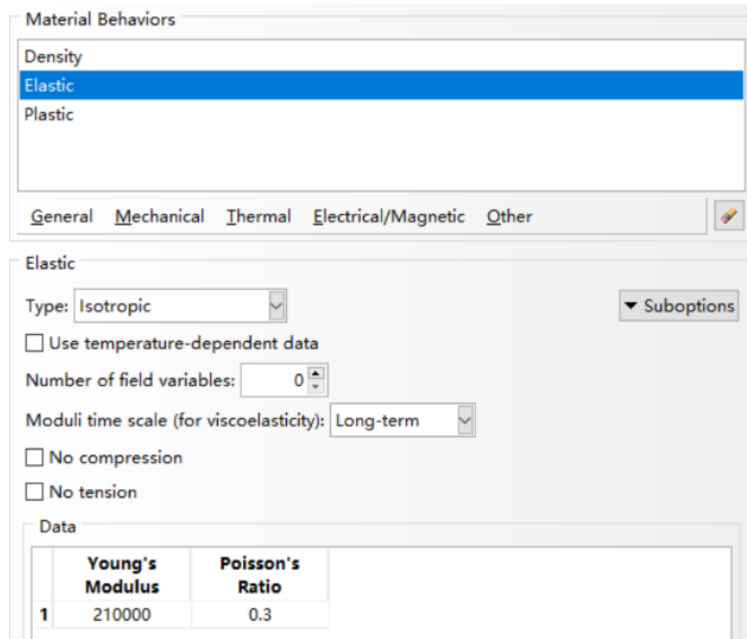


Fig. 2.5 - The material elastic setting of experiment group

Set the plates' material as aluminum (Fig. 2.6, Fig. 2.7)

The mass density of it is 2.7×10^{-9} , and the Young's Modulus is 70000Mpa and the Poisson's Ratio is 0.29.

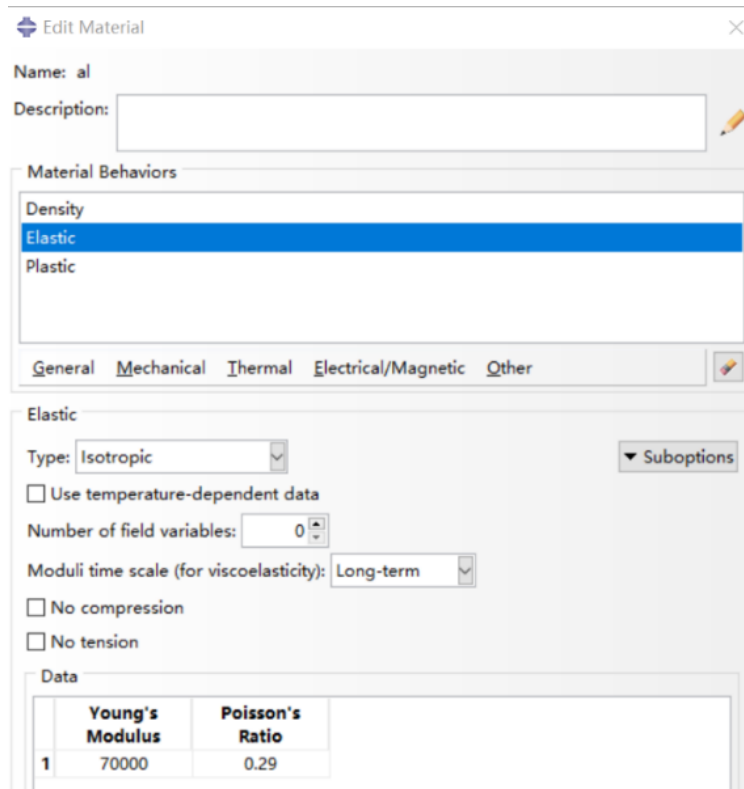


Fig. 2.6 - The material elastic setting of plate

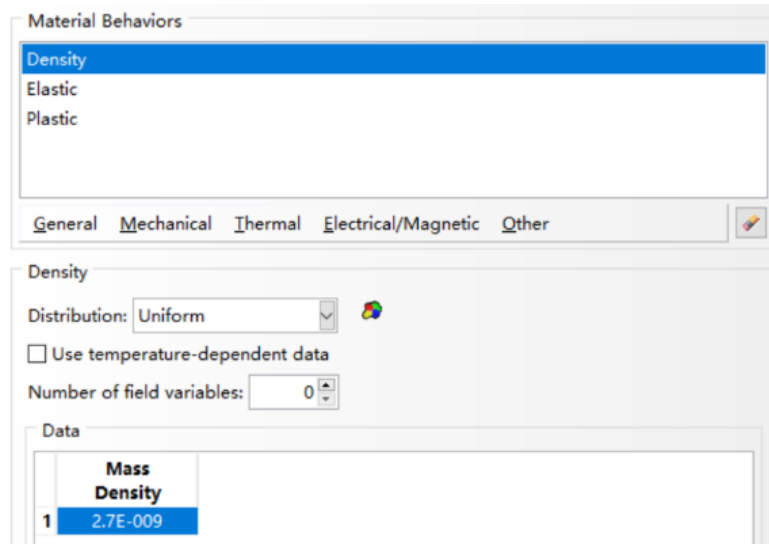


Fig. 2.7 - The material density setting of plate

2.3.3 Loading

Fully restrain the plate at the left end, and apply a coupled concentrated force to the plate at the right end, as shown in the figure below (Fig.2.8, Fig.2.9)

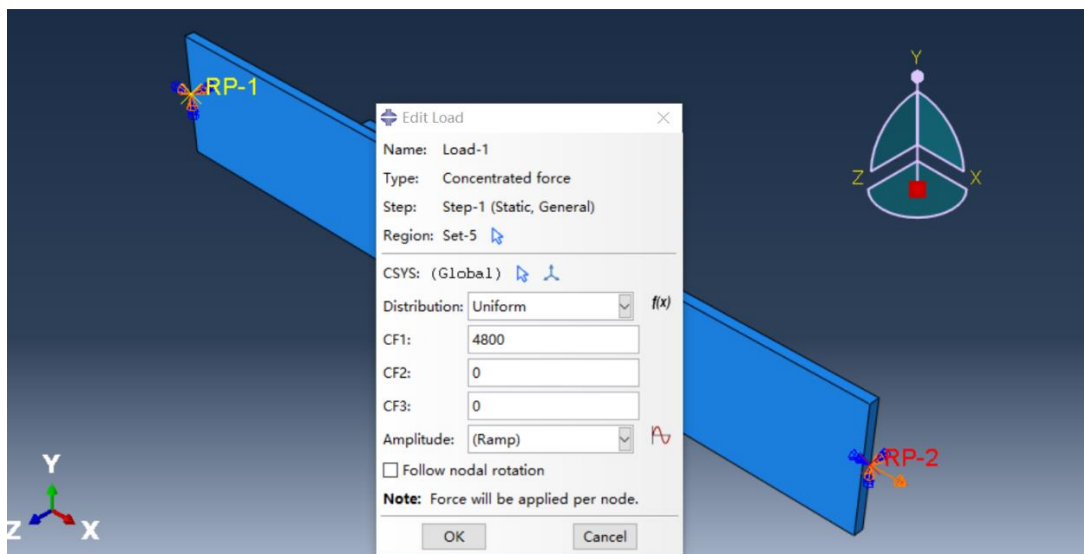


Fig.2.8 - Scheme of concentrated force loading

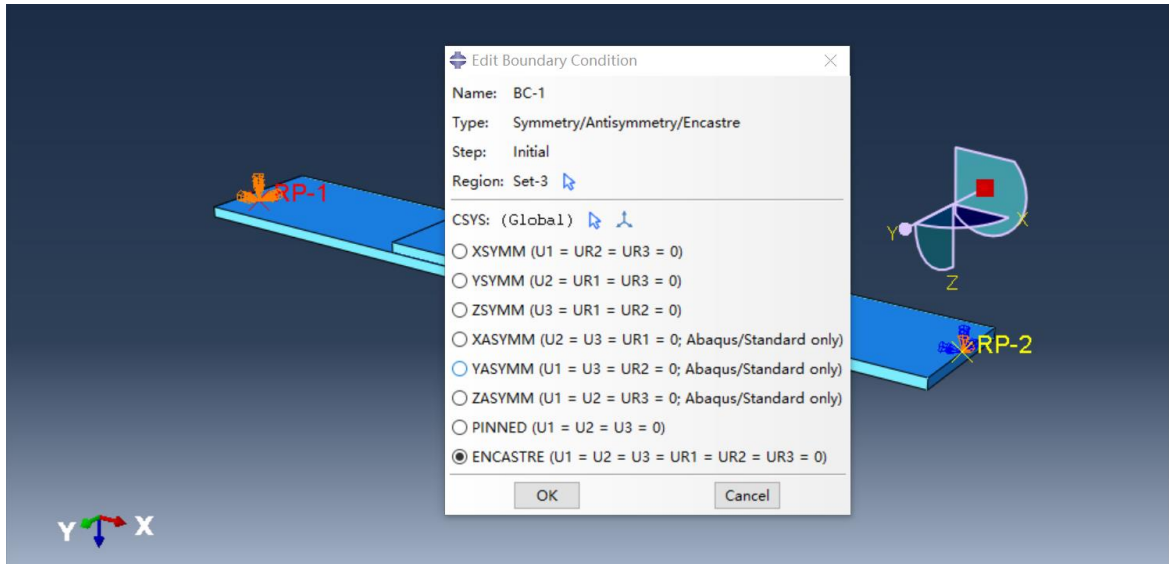


Fig.2.9 - Scheme of fully restrain loading

2.4 Variables: Control groups

2.4.1 Control group 1. Rivet diameter

Figure showed below (Fig.2.10, Fig.2.11) is the three views of the control group 1, as we can see from the figure, the length of the plate is 105mm, width is 24mm, and the thickness of the plate is 2mm. The three rivet holes are 8mm in diameter and 15mm apart.

Compared with the experimental group, the control group has changed the diameter of riveting holes. The other structure and material parameters are consistent with the experimental group. The effect of the aperture size setting on the secondary bending is discussed through the method of controlling variables.

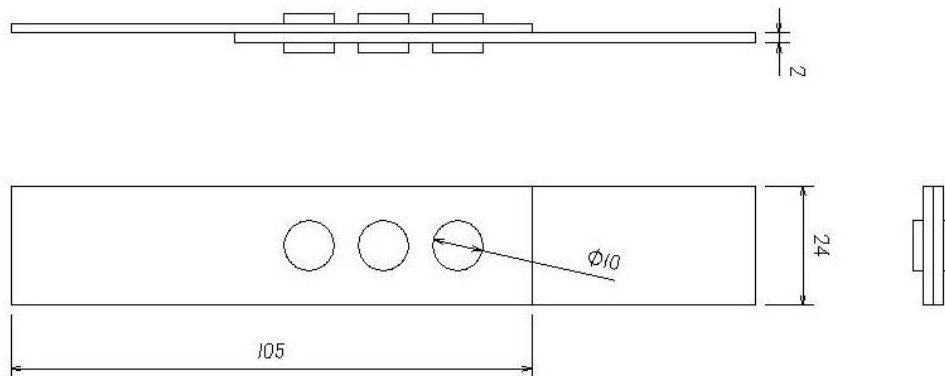


Fig.2.10 - Schematic diagram of riveted control group 1

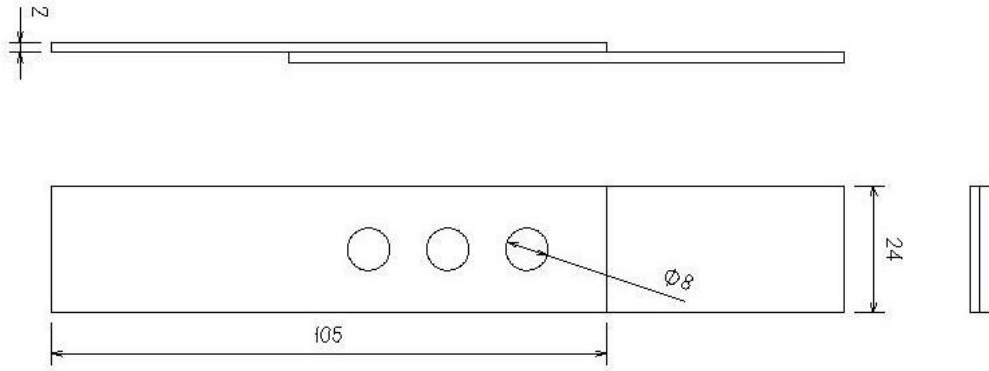


Fig.2.11 - Schematic diagram of control group 1 (Rivet hidden)

2.4.2 Control group 2. Staggered thickness

Figure showed below (Fig.2.12, Fig.2.13) is the views of the control group 2, as we can see from the figure, the length of the plate is 105mm, width is 24mm, and the thickness of the plate is 2mm. The three rivet holes are 5mm in diameter and 15mm apart. The plate has been built with staggered thickness as its shown below.

Compared with the experimental group, the control group has changed the structure of plate. The other structure and material parameters are consistent with the experimental group. The effect of the staggered thickness setting on the secondary bending is discussed through the method of controlling variables.

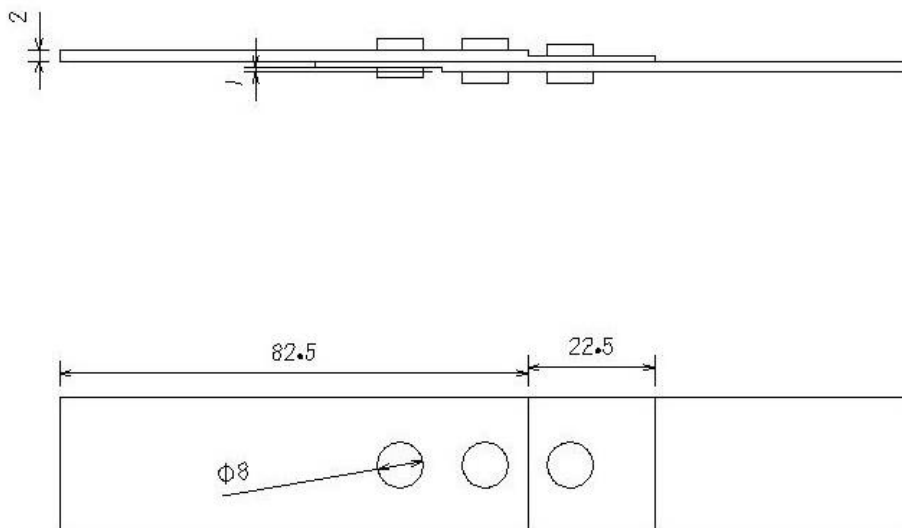


Fig.2.12 - Schematic diagram of riveted control group 2

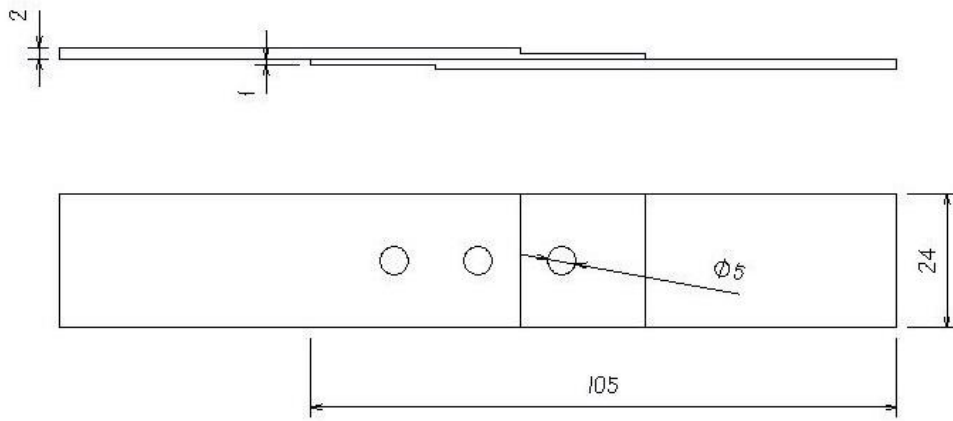


Fig.2.13 - Schematic diagram of control group 2 (Rivet hidden)

2.4.3 Control group 3. Plate thickness

Figure showed below (Fig.2.14, Fig.2.15) is the views of the control group 3, as we can see from the figure, the length of the plate is 105mm, width is 24mm, and the thickness of the plate is 3mm. The three rivet holes are 5mm in diameter and 15mm apart.

Compared with the experimental group, the control group has changed the thickness of the plate. The other structure and material parameters are consistent with the experimental group. The effect of plates' thickness setting on the secondary bending is discussed through the method of controlling variables.

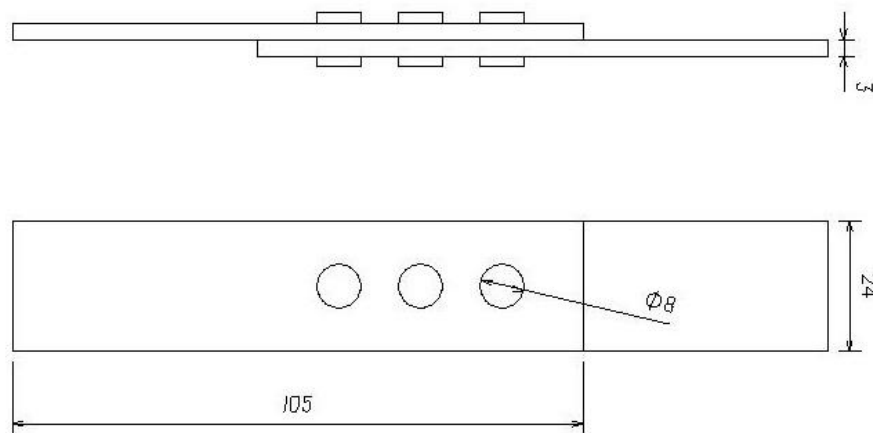


Fig.2.14 - Schematic diagram of riveted control group 3

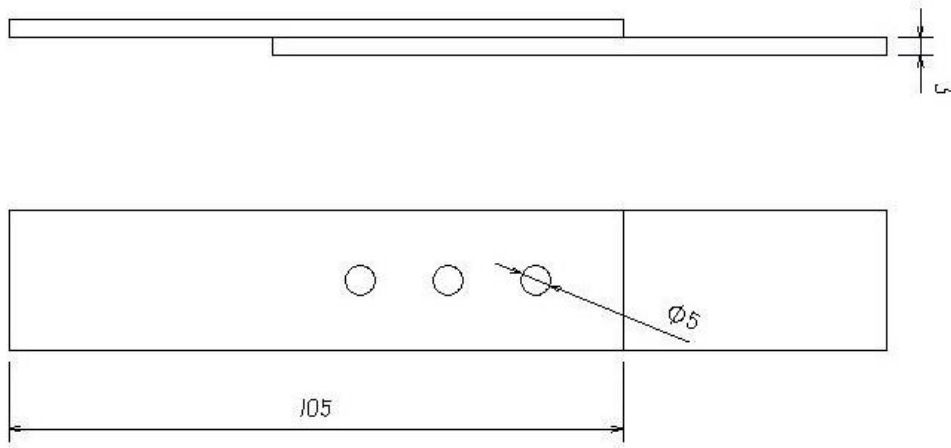


Fig.2.15 - Schematic diagram of control group 3 (Rivet hidden)

2.4.4 Control group 4. Distance between rivets

Figure showed below (Fig.2.16, Fig2.17) is the views of the control group 4, as we can see from the figure, the length of the plate is 105mm, width is 24mm, and the thickness of the plate is 2mm. The three rivet holes are 5mm in diameter and 20mm apart. The plate has been built with staggered thickness as its shown below.

Compared with the experimental group, the control group has changed the distances between the holes. The other structure and material parameters are consistent with the experimental group. The effect of the distance between the holes setting on the secondary bending is discussed through the method of controlling variables.

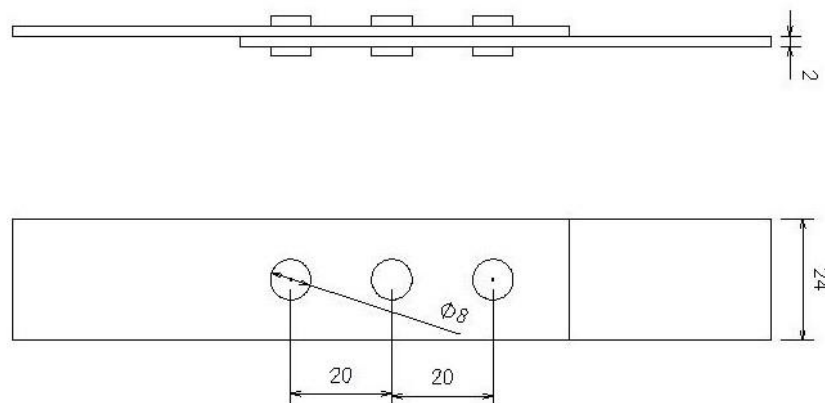


Fig.2.16 - Schematic diagram of riveted control group 4

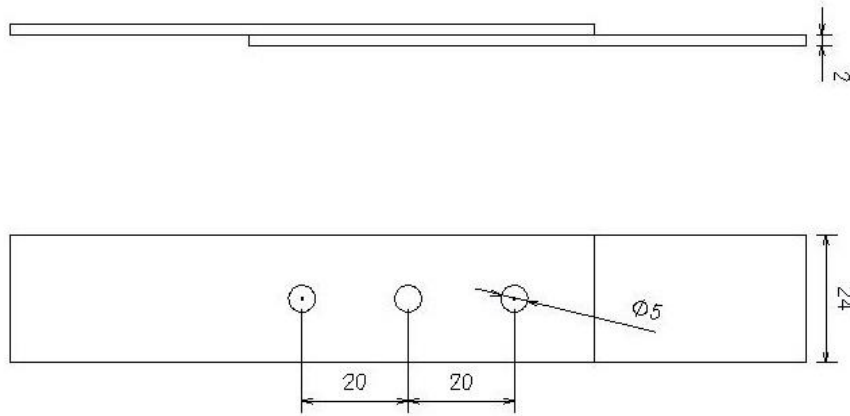


Fig.2.17 - Schematic diagram of control group 4 (Rivet hidden)

2.4.5 Control group 5. Single strap joint

Figure showed below (Fig.2.18, Fig.2.19) is the three views of the control group 5, as we can see from the figure, the length of the plate is 105mm, width is 24mm, and the thickness of the plate is 2mm. The three rivet holes are 5mm in diameter and 15mm apart.

Compared with the experimental group, the control group has changed the number of riveted plates. The other structure and material parameters are consistent with the experimental group.

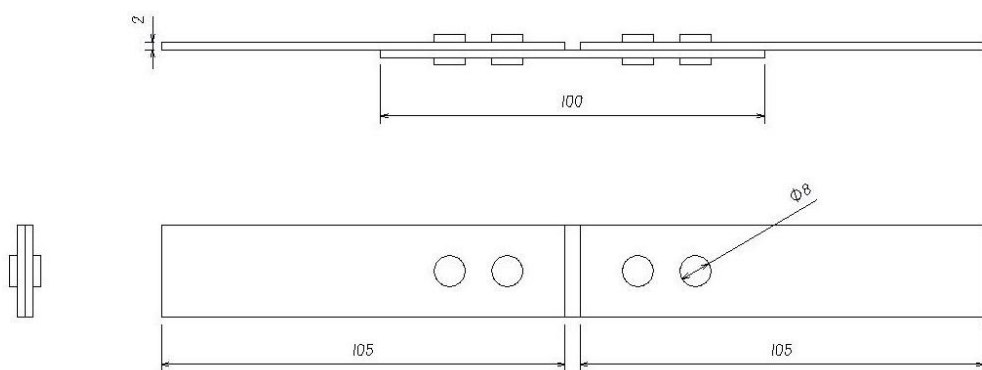


Fig.2.18 - Schematic diagram of riveted control group 5

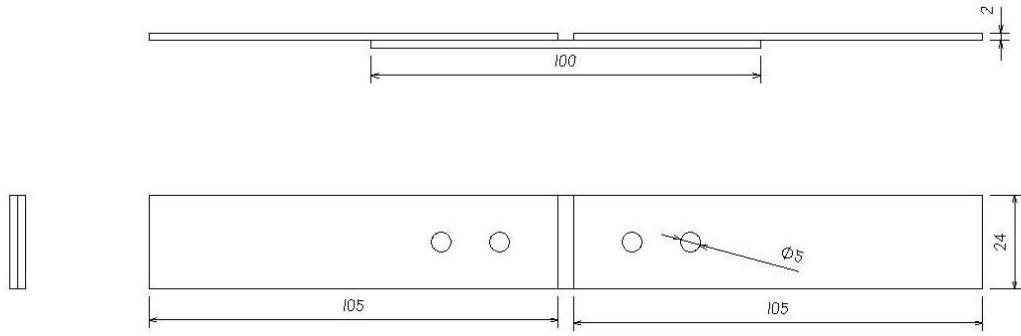


Fig.2.19 - Schematic diagram of control group 5 (Rivet hidden)

2.4.6 Control group 6. Double strap joint

Figure showed below (Fig-2.20, Fig.2.21) is the three views of the control group 6, as we can see from the figure, the length of the plate is 105mm, width is 24mm, and the thickness of the plate is 2mm. The three rivet holes are 5mm in diameter and 15mm apart.

Compared with the experimental group, the control group is double strap joint. The other structure and material parameters are consistent with the experimental group.

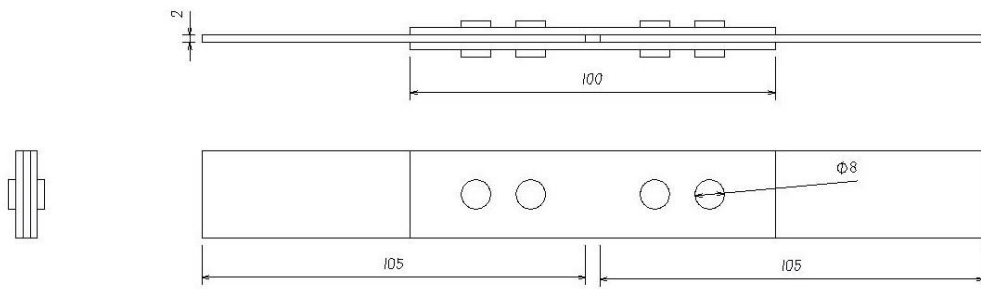


Fig.2.20 - Schematic diagram of riveted control group 6

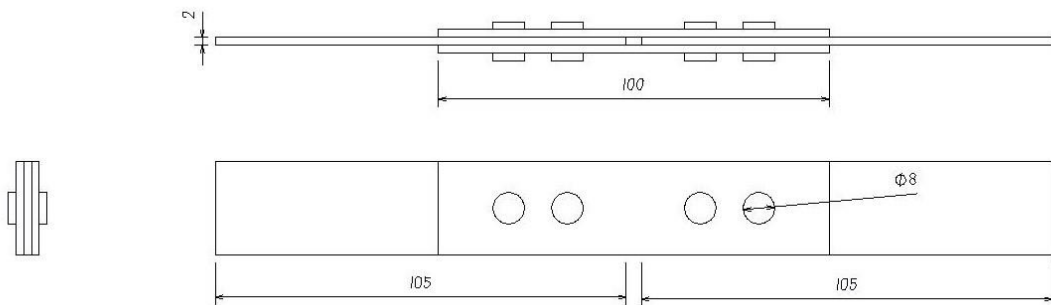


Fig.2.21 - Schematic diagram of control group 6 (Rivet hidden)

2.5 General approach for the evaluation of secondary bending

The contribution of secondary bending is often quantified by the bending factor. And the definition of bending factor k_b has been introduced above. It can be defined as

$$k_b = \frac{S_b}{S} \quad (2.3)$$

Where S_b is the maximum nominal bending stress and S is the nominal tensile stress applied to the joint. Both S_b and S are calculated as the thick part of the table, that is, rivet holes are ignored.

The nominal tensile stress applied to the joint is set before experiment. Through the experimental results of finite element, we can get the data of the maximum nominal bending stress. By comparing the magnitude of the value of bending factor k_b , we can see the effect of the experiment on reducing the effect of secondary bending on aircraft fatigue.

Conclusion to Part 2

The part 2 deals with research procedure. The software for the secondary bending analysis have been selected. The **ABAQUS** which is used in the automotive, aerospace and industrial products industries has been selected as a simple tool for the stress-strain analysis in couple with **CATIA** which is a multi-platform 3D software suite developed by Dassault Systems, including CAD, CAM and CAE.

Preliminary 3D models of the specimens are constructed. All required parameters for the secondary bending analysis are found.

PART 3. SECONDARY BENDING FE ANALYSIS AND RECOMMENDATIONS FOR RIVET JOINTS IMPROVEMENT

3.1 Finite Element Analysis Result of experimental group

After finishing the finite element analysis preprocessing, the finite element model of the experimental group is obtained as shown in the figure below (Fig.3.1)

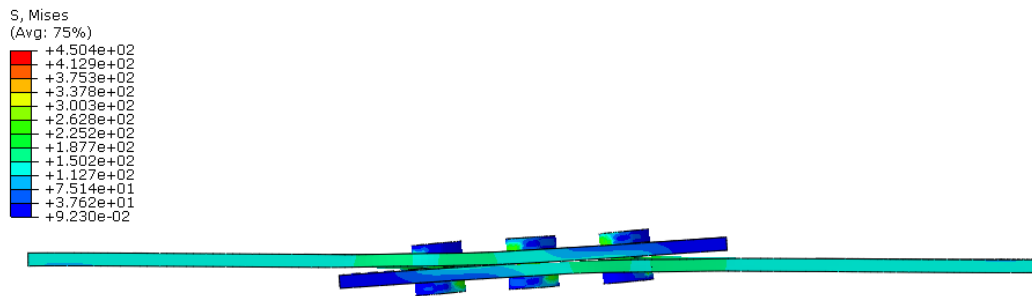


Fig.3.1 - Finite element model of the experimental group

As can be seen from the figure below (Fig.3.2, Fig.3.3), the maximum stress appears at the position of the maximum stress point mentioned in the second part. Stress indicates the distribution of stress in the selected line. True distance means the actual distance (starting at zero) along the path in model space.

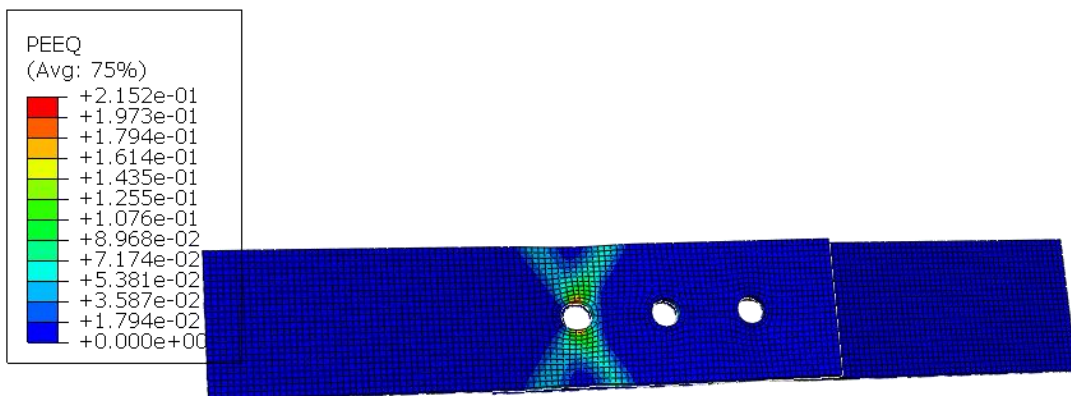


Fig.3.2 - Frontal stress distribution map

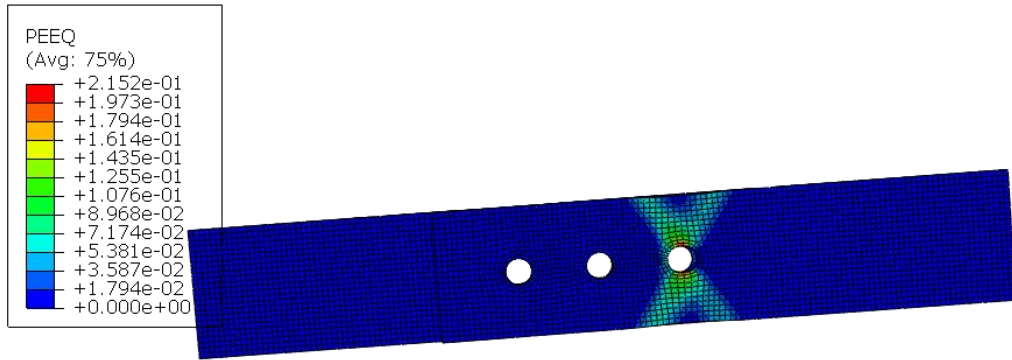


Figure 3.3 - Backside stress distribution map

Use the finite element analysis method to draw a path at the maximum stress, as shown in the figure below (Fig.3.4), calculate the stress on the path through the software, and get the picture of the stress change with the path as shown in the figure (Fig.3.5, Fig.3.6). From the figure we can see that the maximum stress on this path is 218.138Mpa

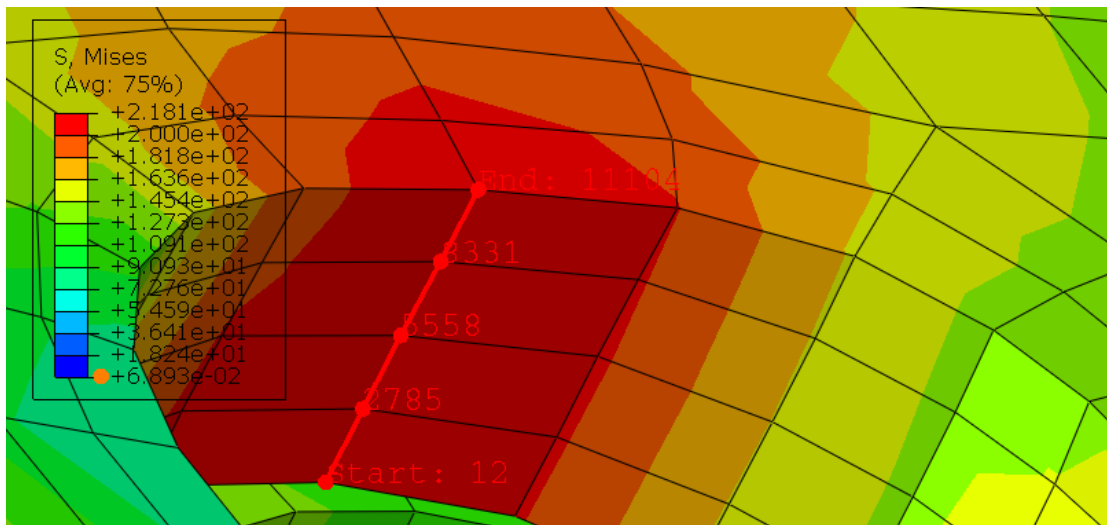


Fig.3.4 - Stress path diagram

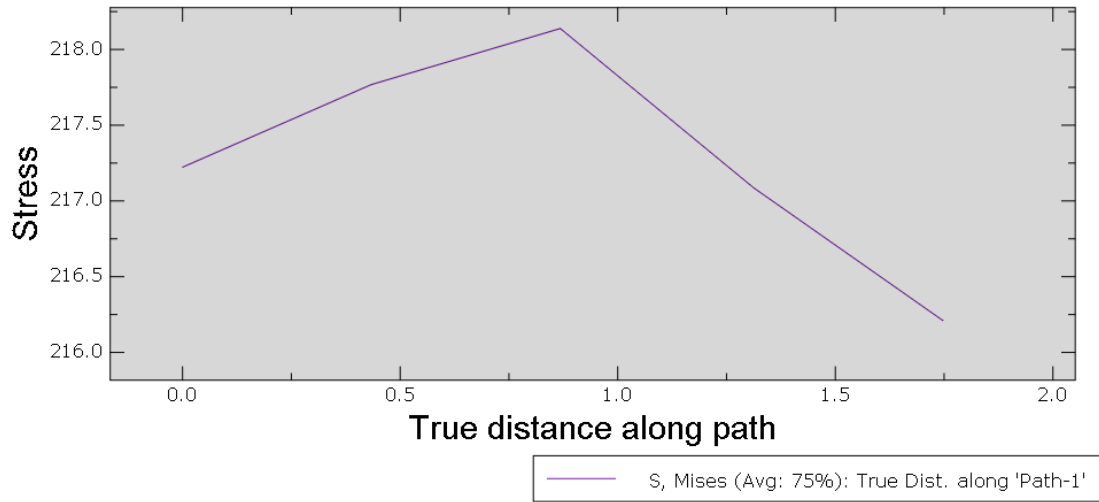


Fig.3.5 - Stress-distance diagram

Edit XY Data ×

Name: experiment group

	Distance along path	Nominal tensile stress
1	0	217.223
2	0.43373	217.768
3	0.86802	218.138
4	1.3125	217.086
5	1.7478	216.209
6		
7		

Fig.3.6 - data from stress- distance diagram

3.2 Finite Element Analysis Results of control groups

3.2.1 Result of control group 1

We have already introduced the differences between control group and experimental group before. Same as the procedure of experimental group, after finishing the finite element analysis preprocessing, the finite element model of the control group is obtained as shown in the figure below (Fig.3.7)

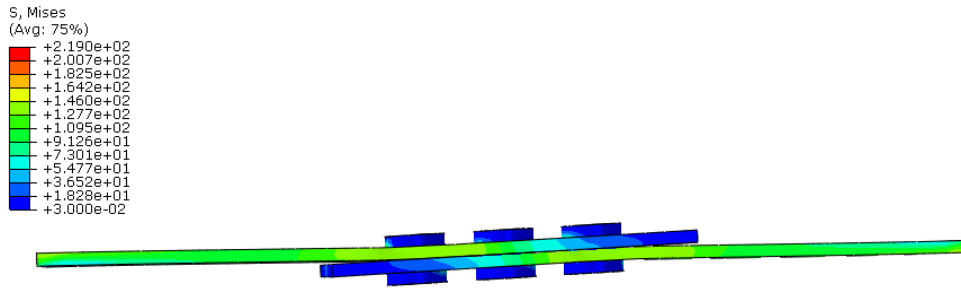


Fig.3.7 - finite element model of the control group1

As can be seen from the figure below (Fig.3.8, Fig.3.9), the maximum stress appears at the position of the maximum stress point.

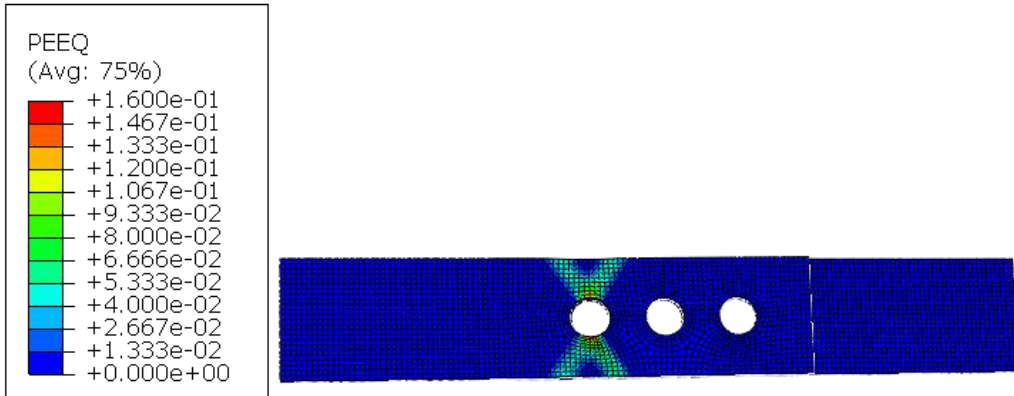


Fig.3.8 - Frontal stress distribution map

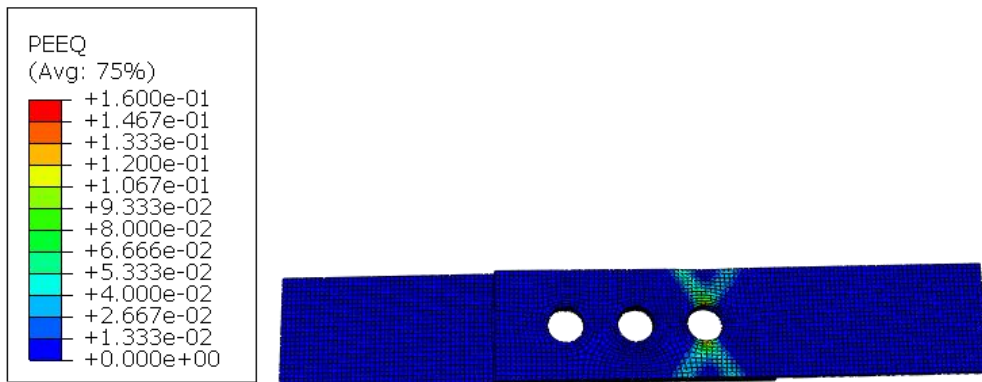


Fig.3.9 - Backside stress distribution map

Use the finite element analysis method to draw a path at the maximum stress, as shown in the figure below (Fig.3.10), calculate the stress on the path through the software, and get the picture of the stress change with the path as shown in the figure(Fig.3.11, Fig.3.12). From the figure we can see that the maximum stress on this path is 197.231Mpa

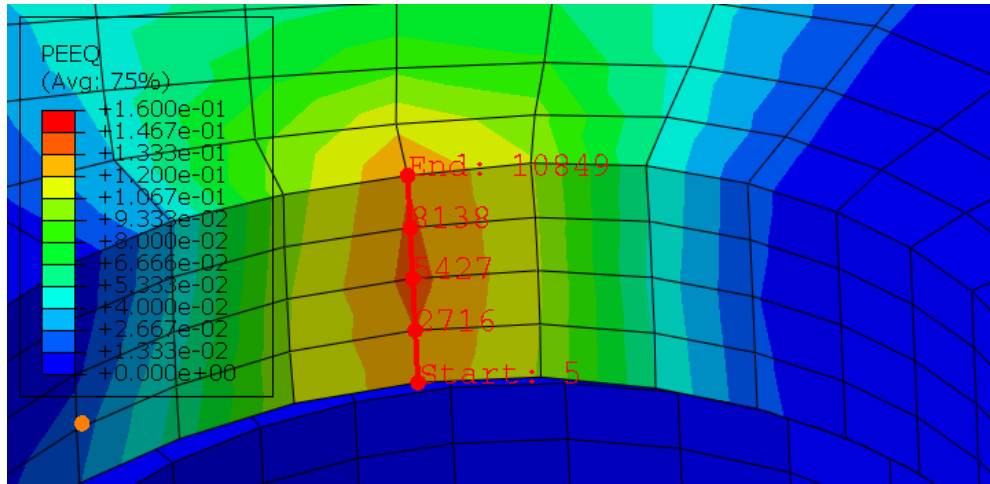


Fig.3.10 - Stress path diagram

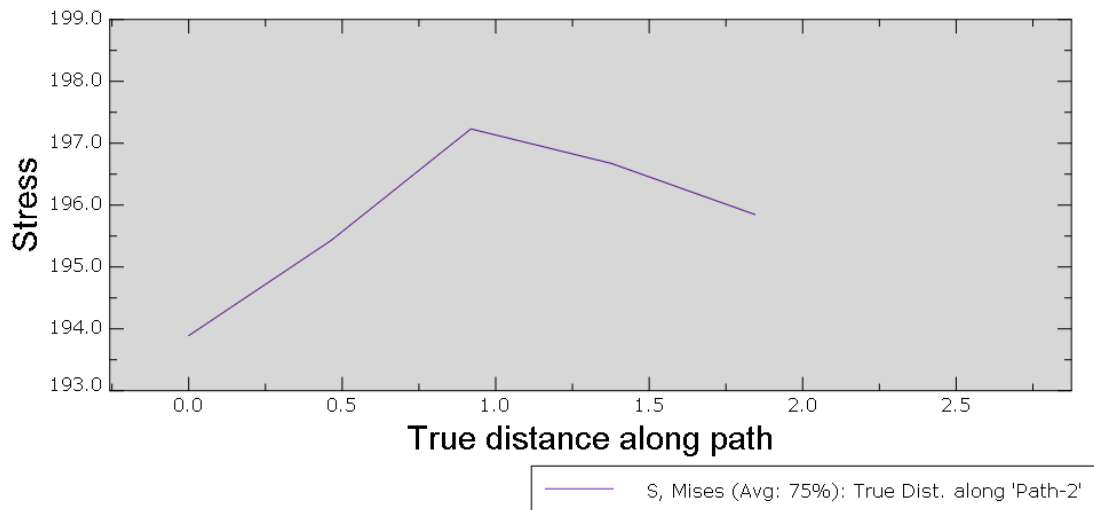


Fig.3.11 - Stress-distance diagram

Edit XY Data		
Name: control group		
	Distance along path	Nominal tensile stress
1	0	193.89
2	0.463303	195.427
3	0.919215	197.231
4	1.37716	196.673
5	1.84504	195.847
6		
7		

Fig.3.12 - data from stress- distance diagram

3.2.2 Result of control group 2

The finite element model of the control group is shown in the figure below (Fig.3.13)

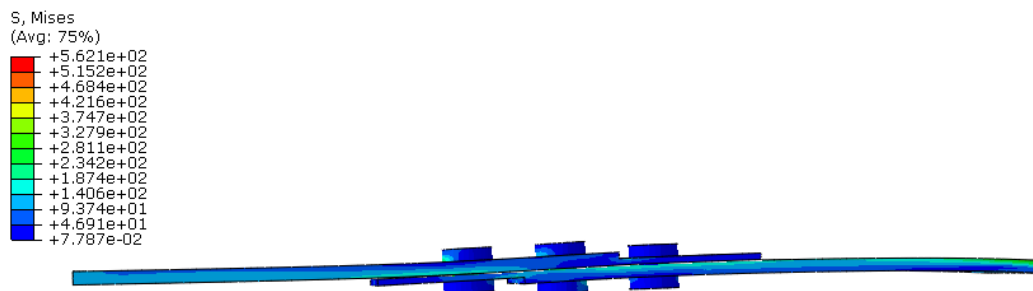


Fig.3.13 - Finite element model of the control group2

As can be seen from the figure below (Fig.3.14, Fig.3.15), the maximum stress appears at the position of the maximum stress point. But it is not shown obviously. So we need to do calculation of the model to see what exactly the number of the maximum stress is.

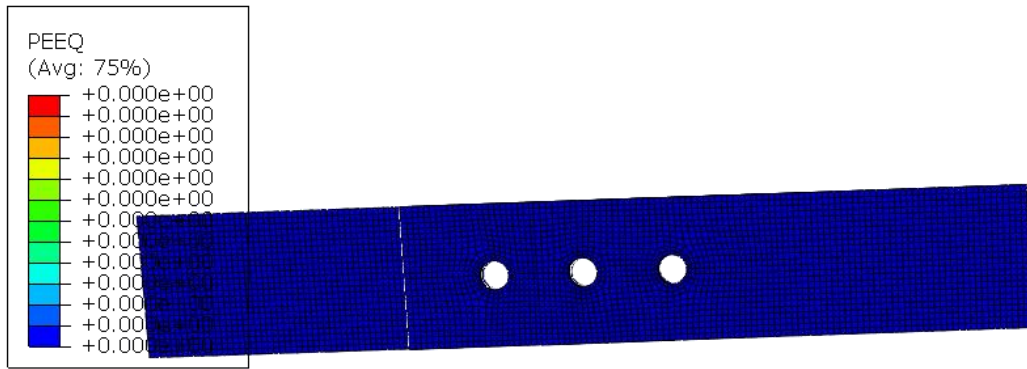


Fig.3.14 - Frontal stress distribution map

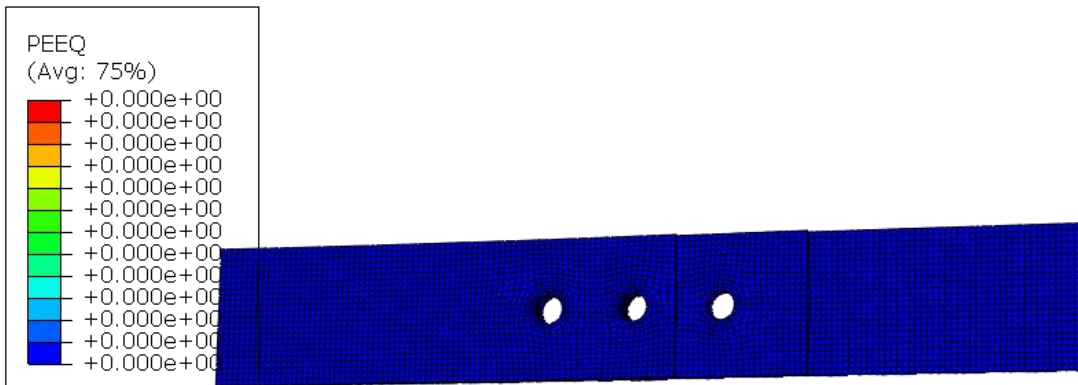


Fig.3.15 - Backside stress distribution map

The path of the maximum stress, as shown in the figure below(Fig.3.16), calculate the stress on the path through the software, and get the picture of the stress change with the path as shown in the figure(Fig.3.17, Fig.3.18). From the figure we can see that the maximum stress on this path is 122.593Mpa

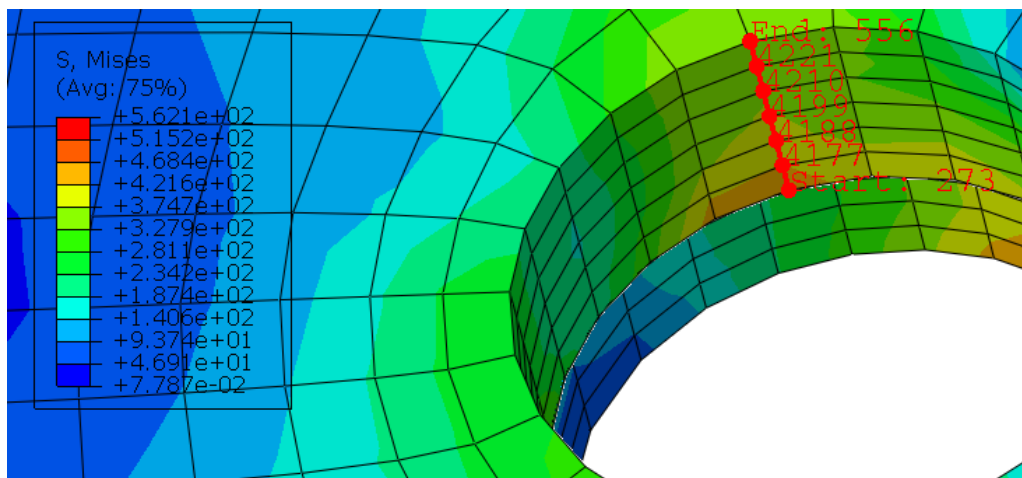


Fig.3.16 - Stress path diagram

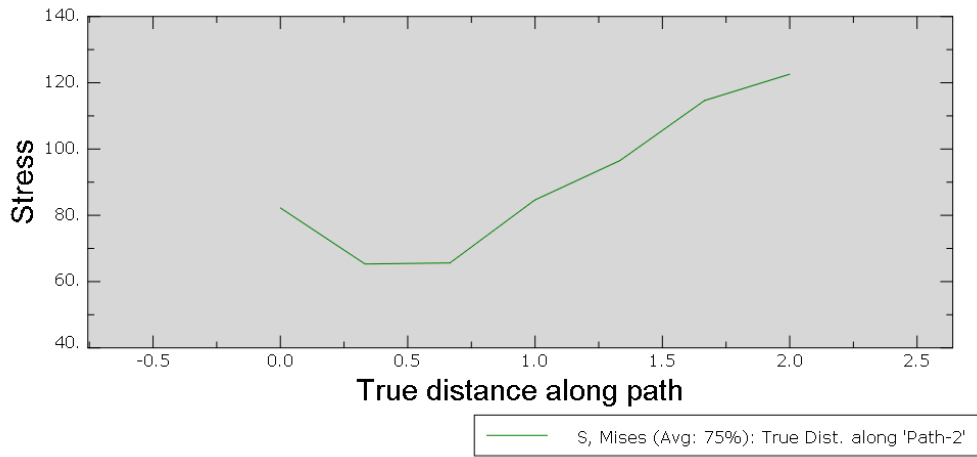


Fig.3.17 - Stress-distance diagram

Edit XY Data

Name: control group 2

	Distance along path	Nominal tensile stress
1	0	82.2356
2	0.332431	65.3068
3	0.665787	65.6306
4	0.998802	84.6011
5	1.33282	96.493
6	1.66543	114.63
7	2.00022	122.593

Fig.3.18 - data from stress-distance diagram

3.2.3 Result of control group 3

The finite element model of the control group is shown in the figure below (Fig.3.19)

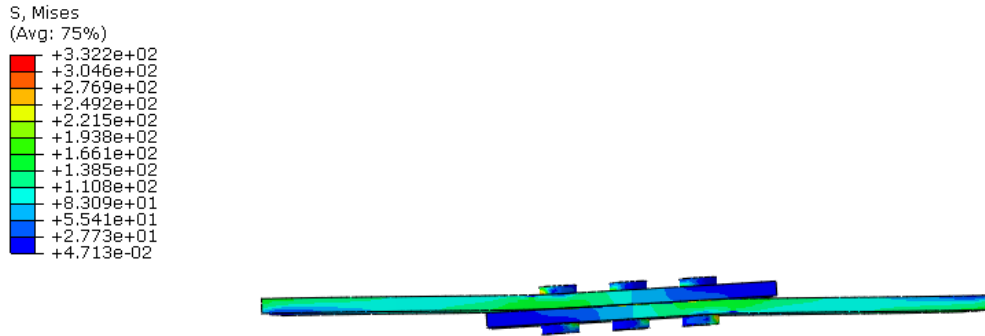


Fig.3.19 - finite element model of the control group 3

As can be seen from the figure below(Fig.3.20, Fig.3.21), the maximum stress appears at the position of the maximum stress point.

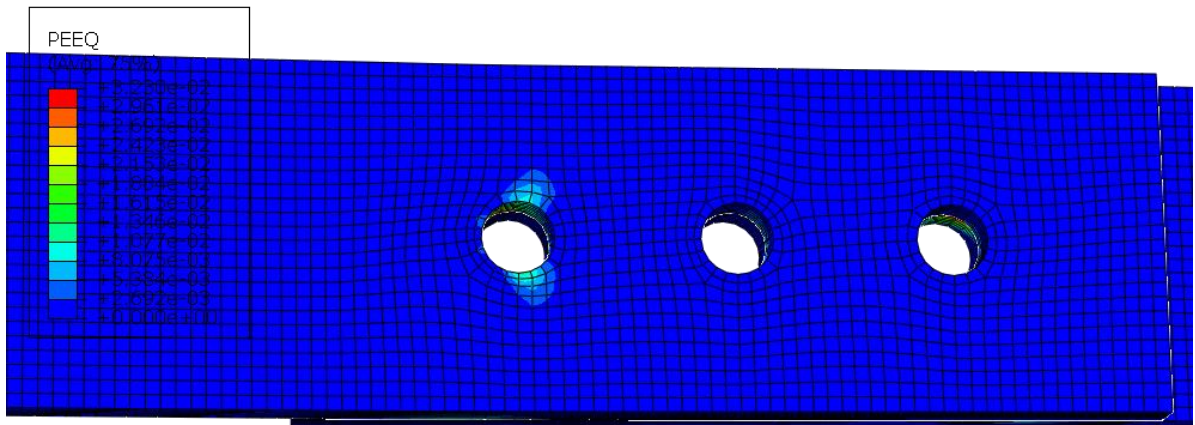


Fig.3.20 - Frontal stress distribution map

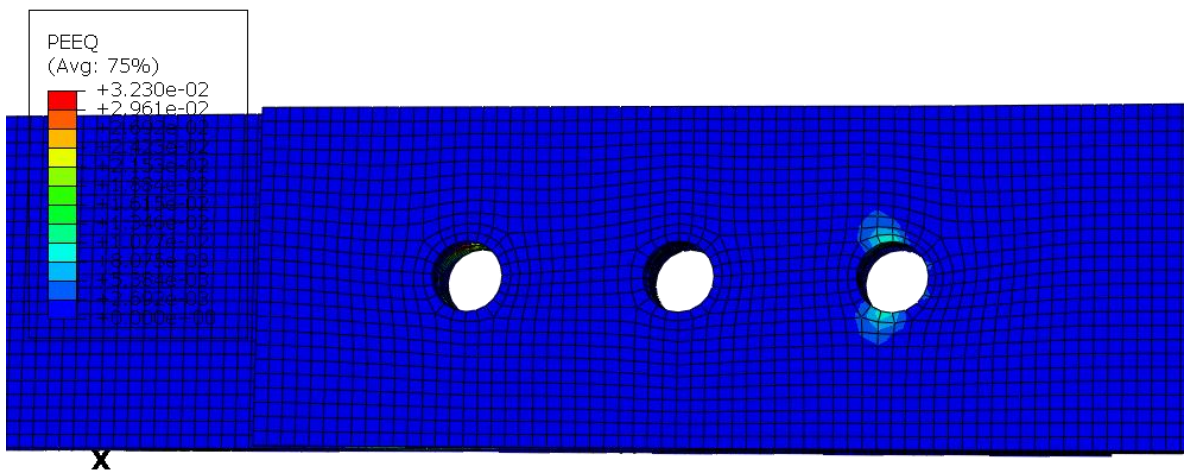


Fig.3.21 - Backside stress distribution map

The path of the maximum stress, as shown in the figure below(Fig.3.22), calculate the stress on the path through the software, and get the picture of the stress

change with the path as shown in the figure(Fig.3.23, Fig.3.24). From the figure we can see that the maximum stress on this path is 139.367Mpa

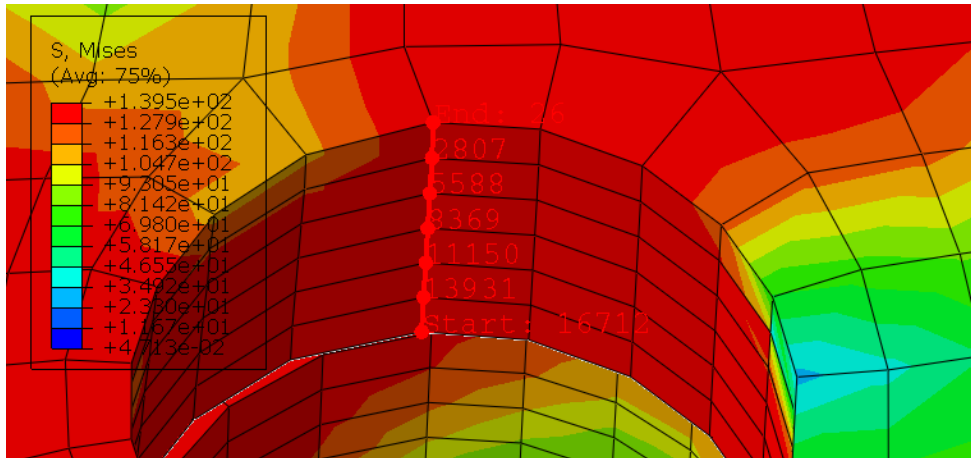


Fig.3.22 - Stress path diagram

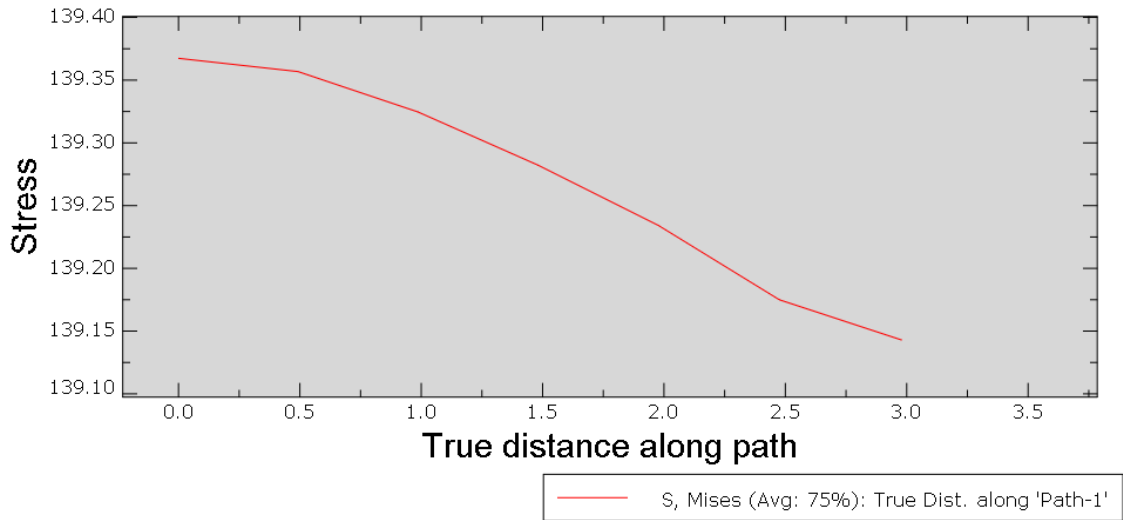


Fig.3.23 - Stress-distance diagram

Edit XY Data		
Name: control group3		
	Distance along path	Nominal tensile stress
1	0	139.367
2	0.492454	139.357
3	0.98613	139.325
4	1.48141	139.282
5	1.97724	139.234
6	2.47537	139.175
7	2.97874	139.143

Fig.3.24 - data from stress- distance diagram

3.2.4 Result of control group 4

The finite element model of the control group is shown in the figure below (Fig.3.25)

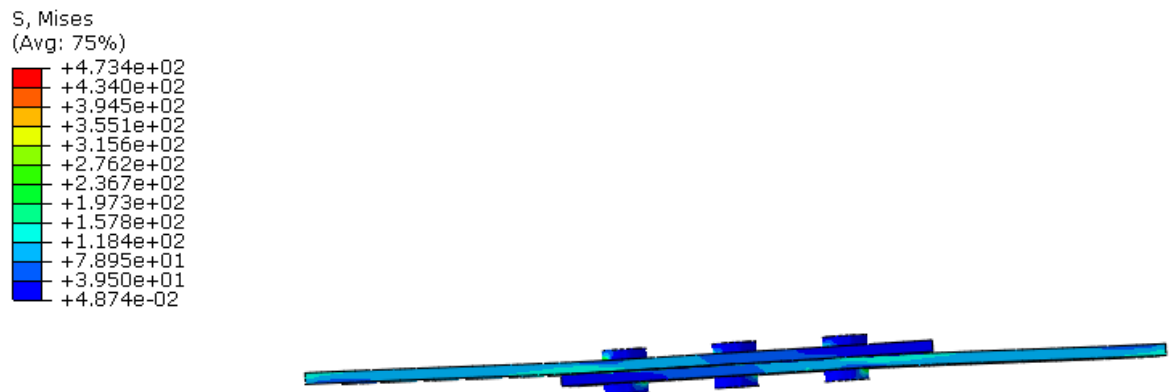


Fig.3.25 - Finite element model of the control group 4

As can be seen from the figure below (Fig.3.26, Fig.3.27), the maximum stress appears at the position of the maximum stress point.

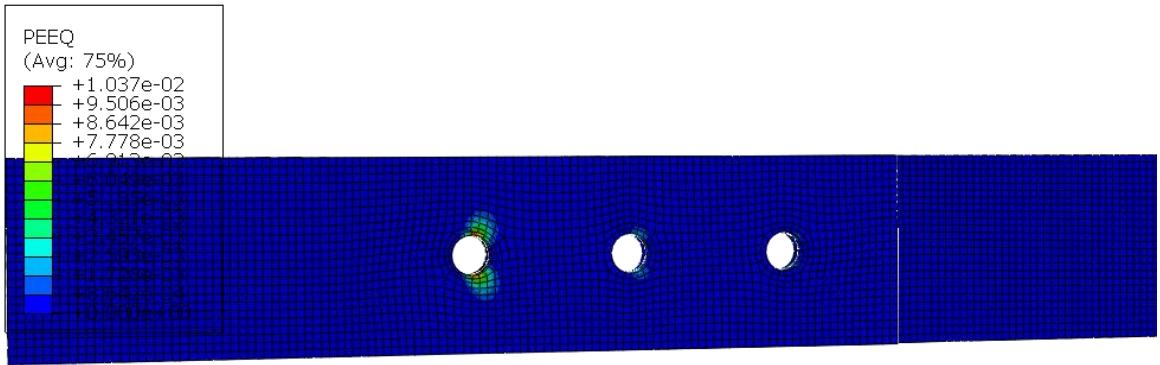


Fig.3.26 - Frontal stress distribution map

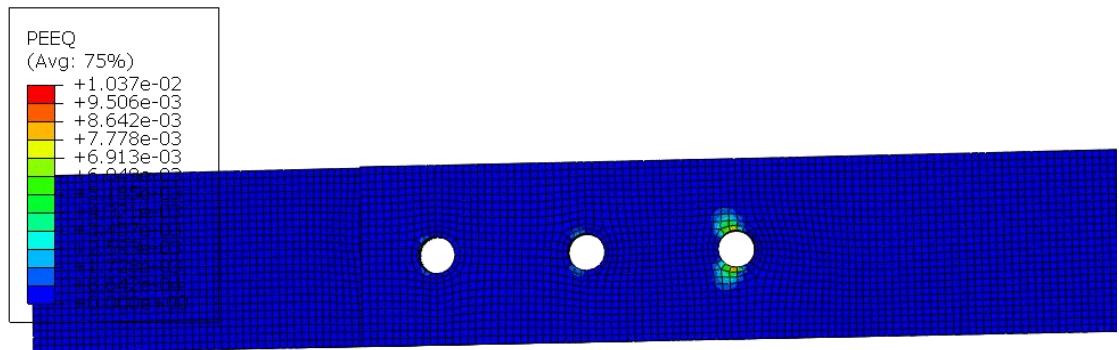


Fig.3.27 - Backside stress distribution map

The path of the maximum stress, as shown in the figure below(Fig.3.28), calculate the stress on the path through the software, and get the picture of the stress change with the path as shown in the figure(Fig.3.29, Fig.3.30). From the figure we can see that the maximum stress on this path is 139.138 Mpa.

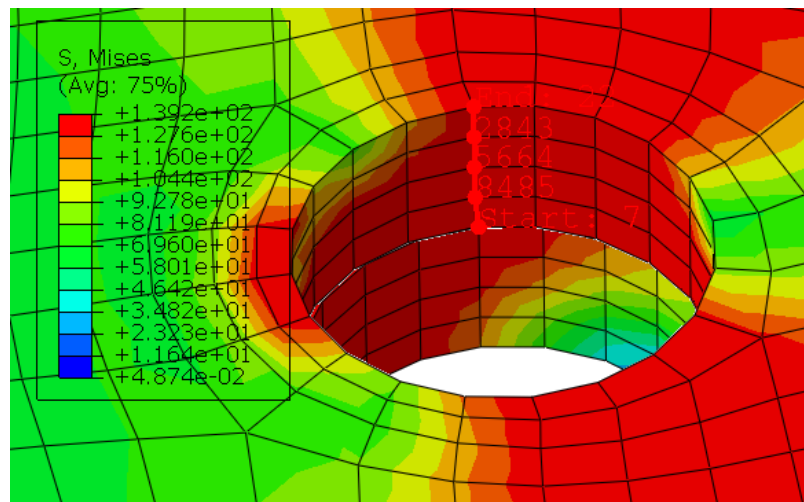


Fig.3.28 - Stress path diagram

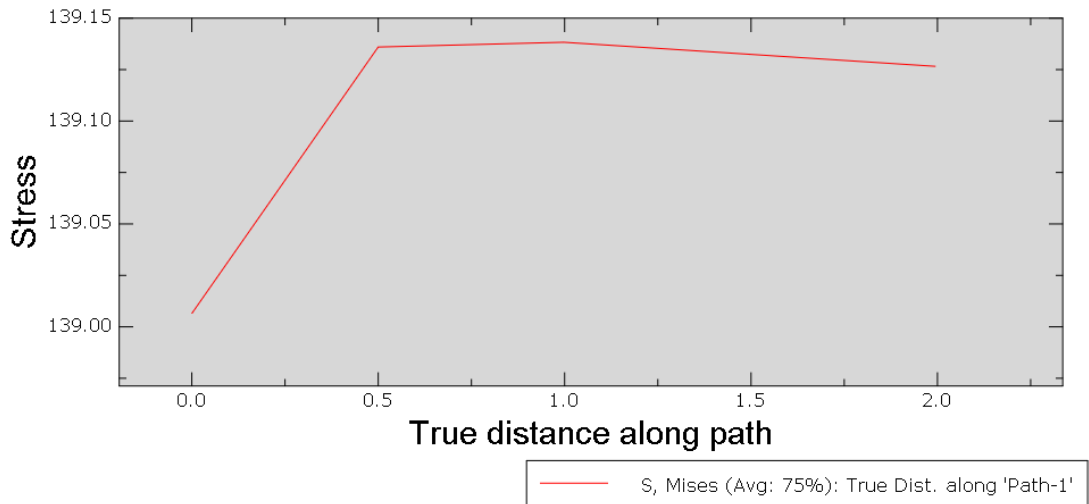


Fig.3.29 - Stress-distance diagram

Edit XY Data

Name: control group 4

	Distance along path	Nominal tensile stress
1	0	139.006
2	0.499918	139.136
3	0.997605	139.138
4	1.49553	139.132
5	1.99464	139.127
6		
7		

Fig.3.30 - Data from stress- distance diagram

3.2.5 Result of control group 5

The finite element model of the control group is shown in the figure below (Fig.3.31)

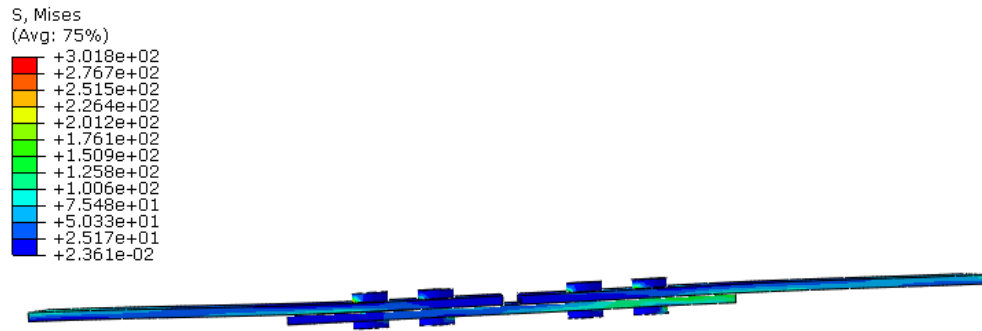


Fig.3.31 - Finite element model of the control group 5

As can be seen from the figure below(Fig.3.32), the maximum stress appears at the position of the maximum stress point.

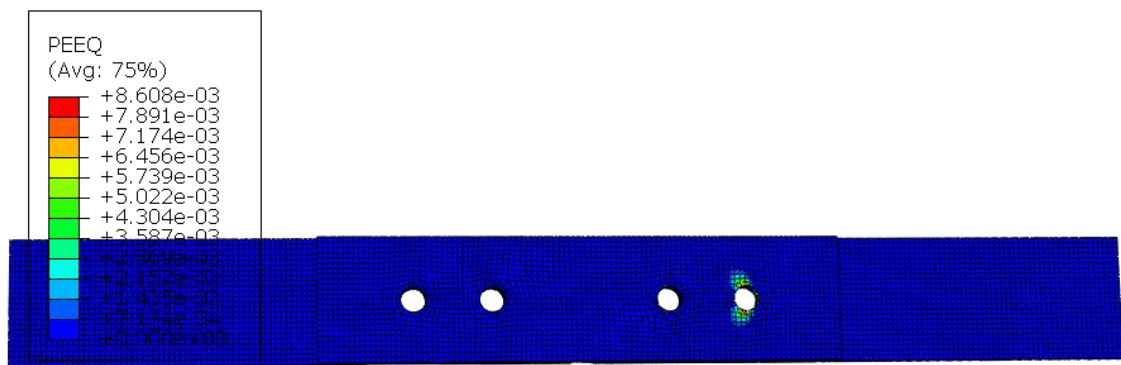


Fig.3.32 - Frontal stress distribution map

The path of the maximum stress, as shown in the figure below(Fig.3.33), calculate the stress on the path through the software, and get the picture of the stress change with the path as shown in the figure(Fig.3.34, Fig.3.35). From the figure we can see that the maximum stress on this path is 139.127Mpa

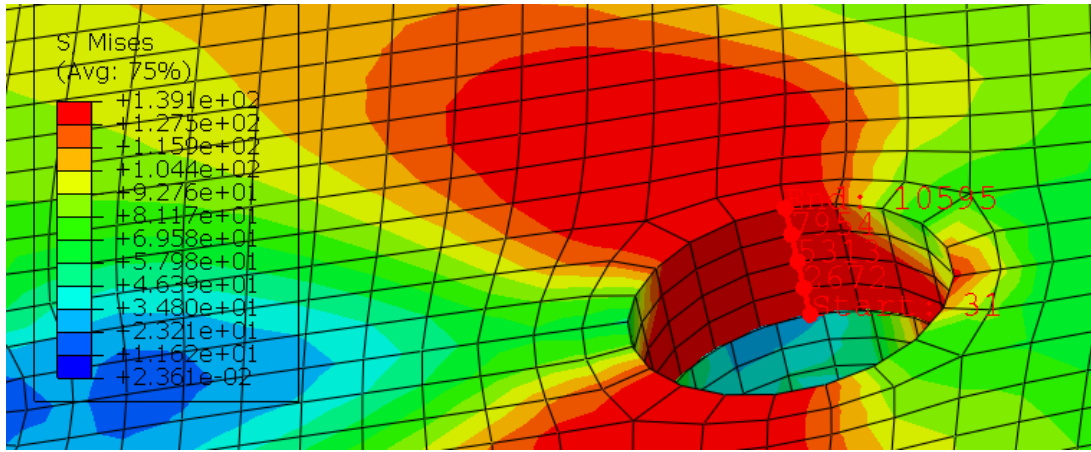


Fig.3.33 - Stress path diagram

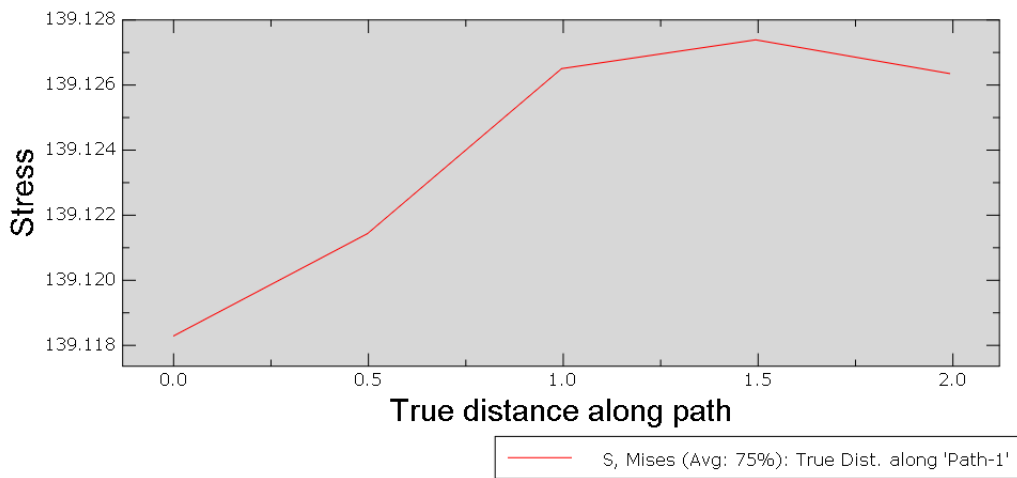


Fig.3.34 - Stress-distance diagram

Edit XY Data

Name: control group5

	Distance along path	Nominal tensile stress
1	0	139.118
2	0.497727	139.121
3	0.995624	139.126
4	1.49381	139.127
5	1.99259	139.126
6		
7		

Fig.3.35 - Data from stress- distance diagram

3.2.6 Result of control group 6

The finite element model of the control group is shown in the figure below (Fig.3.36)

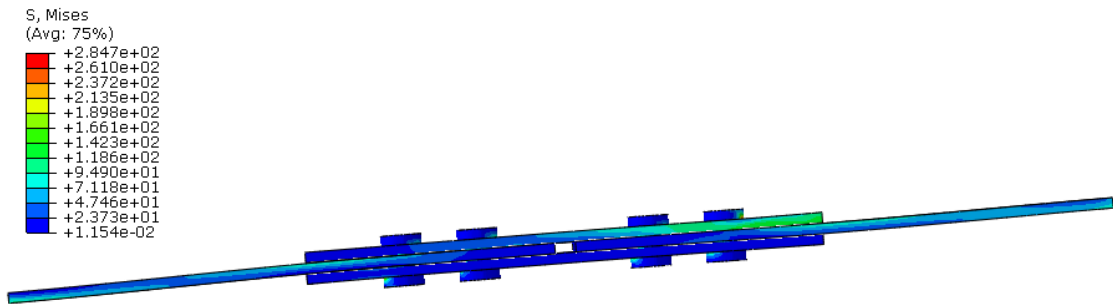


Fig.3.36 - Finite element model of the control group 6

As can be seen from the figure below(Fig.3.37, Fig.3.38), the maximum stress appears at the position of the maximum stress point. But it is not shown obviously. So we need to do calculation of the model to see what exactly the number of the maximum stress is.

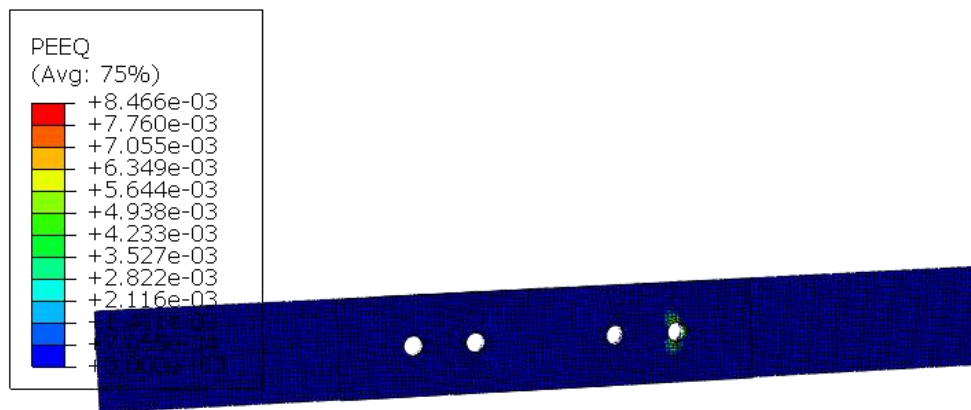


Fig.3.37- Frontal stress distribution map

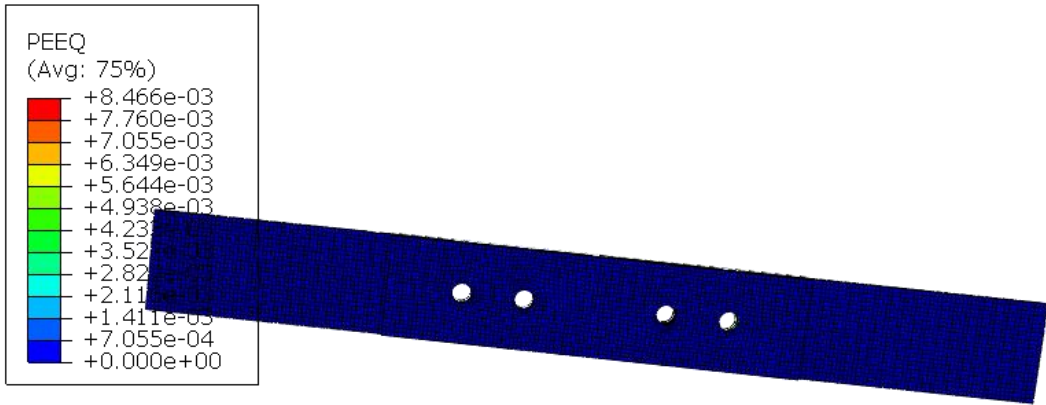


Fig.3.38 - Backside stress distribution map

The path of the maximum stress, as shown in the figure below (Fig.3.39), calculate the stress on the path through the software, and get the picture of the stress change with the path as shown in the figure (Fig.3.40, Fig.3.41). From the figure we can see that the maximum stress on this path is 21.971 Mpa.

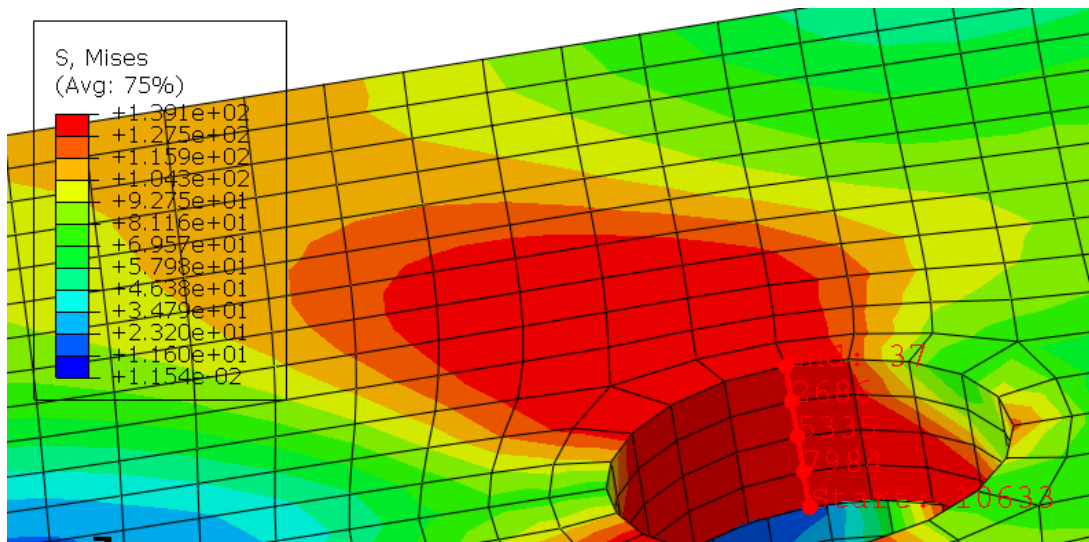


Fig.3.39 - Stress path diagram

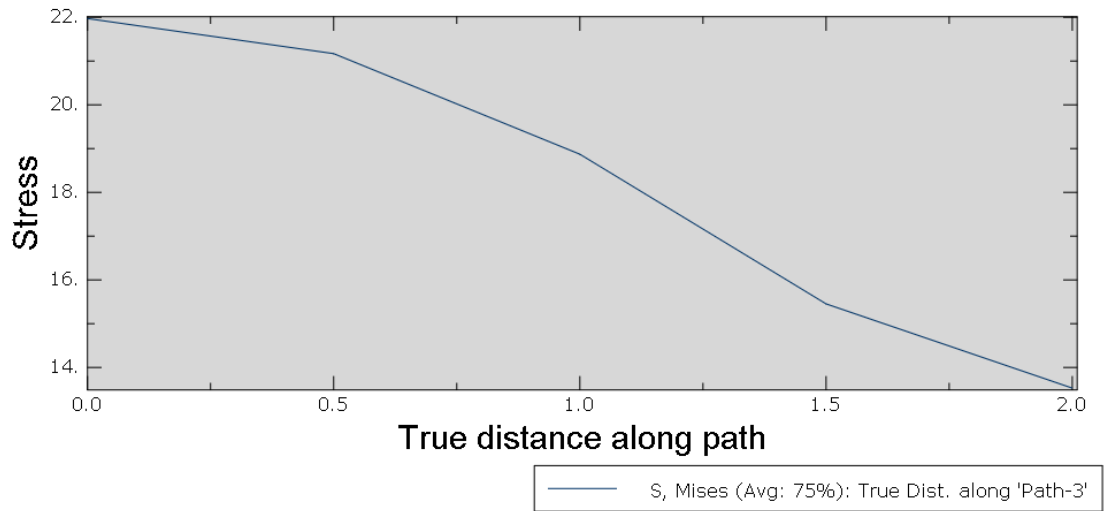


Fig.3.40 - Stress-distance diagram

Edit XY Data ×

Name: control group

	Distance along path	Nominal tensile stress
1	0	21.971
2	0.499952	21.1695
3	0.999859	18.872
4	1.50005	15.4521
5	1.99996	13.528
6		
7		

Fig.3.41 - data from stress- distance diagram

3.3 Calculation of bending factor

Secondary bending can be described with bending factor k_b , The calculation method of the second bending can be defined as:

$$k_b = \frac{S_b}{S} \quad (3.1)$$

Where S_b is the maximum nominal bending stress and S is the nominal tensile stress applied to the joint. Both S_b and S are calculated as the thick part of the table, that is, rivet holes are ignored.

The maximum bending moment occurs at the eccentricity, that is, the fastener row. For loop joints with more than two rivet rows, the position of the maximum bending moment is always located in the outer row.

With the help of Abaqus, obtained the exact value of S_b (nominal bending stress), S is the remotely applied tensile stress, it depends on the stress set before FEA, and can be calculated.

With the correct value of S_b and S , we can calculate the value of K_b of experimental group and all control groups.

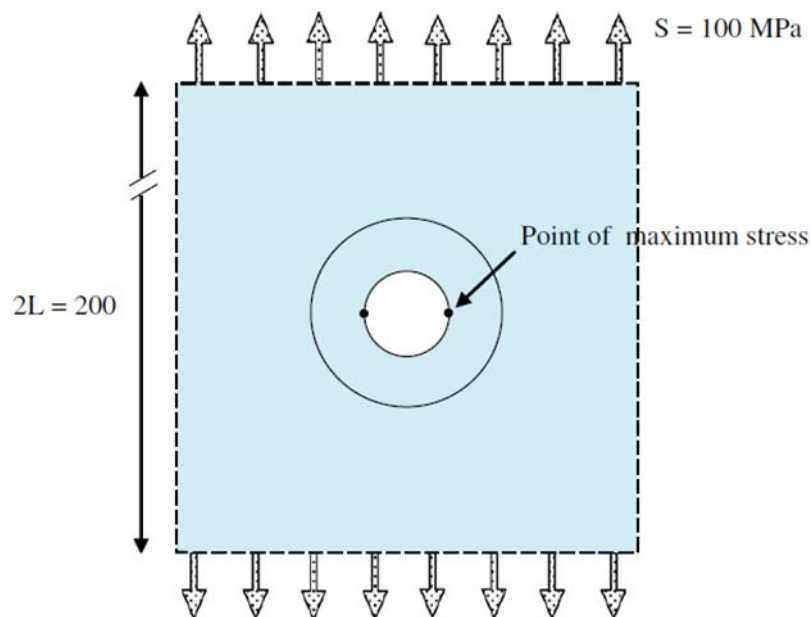


Fig.3.42 - The point of maximum stress

As the article written by Schijve, J. (reference 5) The point of maximum stress is shown above (Fig.3.42). Through the finite element calculation results, we get the value of the maximum force.

S can be calculated as:

$$S = \frac{F}{A} \quad (3.2)$$

F -the force applied on the plate before FEA

A-The area of the pressure acting surface

S_b can be obtained by FEA calculation results.

Use the data of the experimental group as an example:

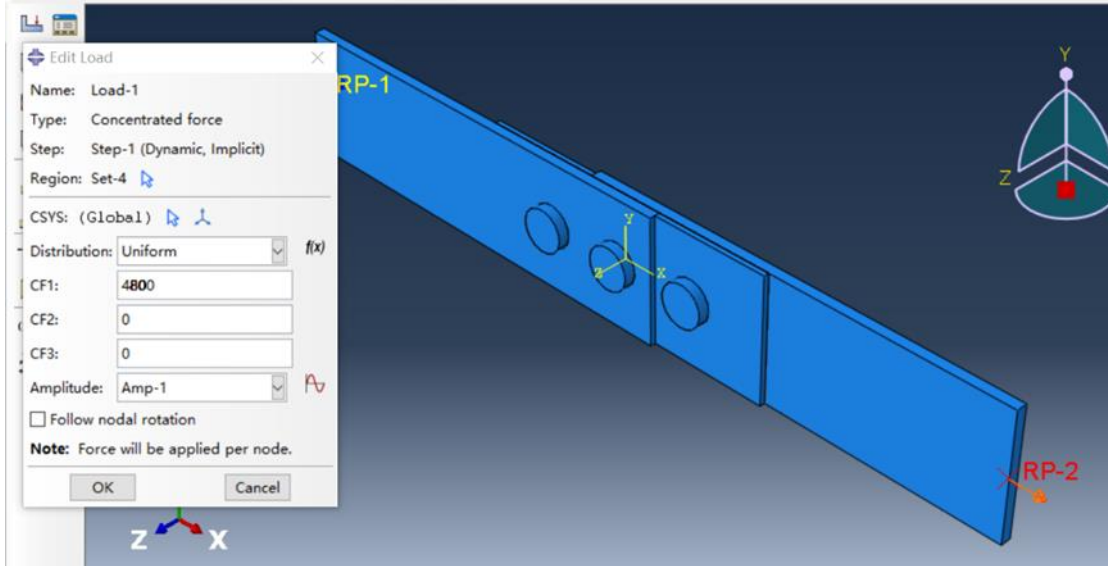


Fig.3.43 - Force applied on plate area

The plate Forced area is 24mm *2mm and the force applied on the plate area is set as 4800N(Fig.3.43).

Follow the formula 3.2 the S can be calculated as $4800N/24mm*2mm=100Mpa$

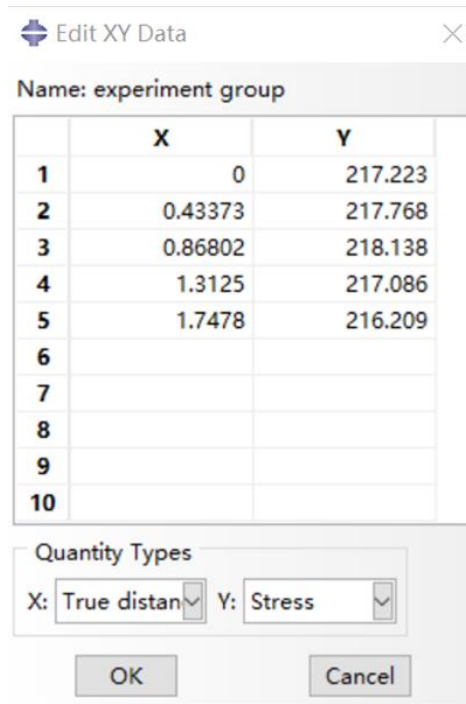


Fig.3.44 - FEA result of experimental group

Through the FEA calculation result of experimental group shown above (Figure 3.44), the maximum stress appeared is 218.138 Mpa.

With the formula 3.1, the K_b is calculated as $218.138/100 \approx 2.18$.

In all the control groups, through the force area and applied pressure control, all the data of S is set as 100Mpa.

The following table (Table 3.1) shows the maximum stress values for all control groups:

Table 3.1-The maximum stress values for all control groups

Variables	Values(MPa)
1	197.231
2	122.593
3	139.367
4	139.138
5	139.127
6	21.971

From table 3.1 and the value of S, the k_b value of all control groups can be calculated as table below (table 3.2).

Table 3.2 - k_b - Value of all control groups

Variables	Values
1	1.97
2	1.23
3	1.39
4	1.39
5	1.39
6	0.22

3.4 Results analysis

Compare the results of all the control groups with the experimental group, all the bending factor data are significantly reduced. This shows that the conditions set in the experiment have a certain mitigation effect on the influence of the secondary bending, and the expected effect of the experiment has been initially achieved.

In the control group 1, the pore size was changed, the bending factor k_b is 1.97, smaller than the value of experimental group. In the control group 2, a staggered plate structure was used, the bending factor k_b is 1.23, smaller than the value of experimental group. In the control group 3, the thickness of the plate was increased, the bending factor k_b is 1.39, smaller than the value of experimental group. In control group 4, the distance between riveting holes increased, the bending factor k_b is 1.39, smaller than the value of experimental group. In the control group 5, a single-band joint was used, the bending factor k_b is 1.39, smaller than the value of experimental group. In the control group 5, a double-band joint was used, this is a non-eccentric structure, so the bending factor k_b is 0.22, Almost no secondary bending.

3.5 Recommendations for rivet joints improvement

3.5.1 Increase the size of the Rivet

Control group 1 shows the k_b results for lap joints with larger hole sizes, as shown in Figure 3.2a. Compared with the smaller hole size lap board of the experimental group, the increase in the hole diameter slightly reduces the bending coefficient. The larger hole size reduces secondary bending, which may benefit the fatigue strength of the lap joint.

3.5.2 Set the lap joint with a staggered sheet thickness

Control group 2 shows the k_b result of the lap joint with staggered plate thickness shown in Figure 3.3a. Compared with the usual constant thickness of the lap joint sheet, the staggering of the thicknesses again reduces the bending coefficient slightly. This decrease may be related to a slight decrease in the bending stiffness of the overlapping area of the joint. However, the main reason for the staggered thickness configuration is related to the load transmission of the three rows of rivets. The load transfer mainly occurs in the outer row, while the inner row transfers less. Larger overlap reduces secondary bending, which may benefit the fatigue strength of lap joints.

3.5.3 Increase plate thickness

In the control group 3, as the thickness of the laminate increases, the secondary bending effect of the laminate becomes serious. The entire laminate has this behavior, and the increase in the thickness of the laminate will increase the local bending stress of the laminate. For this reason, the increase in the thickness of the laminate will increase the bending stress, but the secondary bending effect at the joint slows down. This is the purpose of our experiment.

3.5.4 Increase the distance between the rivets

In the control group 4, the distance between the holes is increased, and the larger distance between the rivet rows of the lap joint means that the bending coefficient k_b is reduced. Some results in the k_b calculation results of the control group 4 illustrate this point. Increasing the rivet row spacing from 15 mm to 20 mm reduces the k_b , which may be beneficial for fatigue performance. In any case, small line spacing should be avoided.

3.5.5 Design a symmetrical and non-eccentric structure

The control group 5 is a single-band joint, which can also be regarded as two lap joints in series. The control group 6 is a double-belt joint. In this completely symmetrical structure, there is no eccentricity and no secondary bending will occur. The best results apply to symmetrical double-belt joints without eccentricity. The strap connector with two staggered straps comes next. Since the short strap has a relatively large thickness, the secondary bending of the joint is limited. Lap joints and single-strap joints show higher bending coefficients.

Conclusion to Part 3

In the third part, the finite element calculation results of the experimental group and all the control groups are analyzed, and the second bending characterization coefficient k_b of all the experiments is obtained, and the results of the experimental group and the control group are compared, on the basis of the comparative experiment result, the riveting improvement suggestions are given.

PART 4. ENVIRONMENTAL PROTECTION

4.1 Requirements towards aircraft safety in terms of its construction in China

Considering that this article mainly discusses the structural optimization of aircraft riveted joints, this chapter mainly quotes the structural safety requirements and clauses of the airworthiness standards for transport aircraft in China's civil aviation regulations. However, with the advancement of aviation technology, the development of aviation manufacturing and air transportation, and the deepening of people's understanding of aviation safety, the airworthiness standards themselves are constantly evolving and updating. In recent years, there have been new developments in the international airworthiness research and standard formulation of transport aircraft.

In terms of the load requirements of the design structure, the strength requirements are specified by the limit load (the maximum load expected in service) and the ultimate load (the limit load multiplied by the specified safety factor). The air, ground, and water loads must be balanced with the inertial force that takes into account each mass item of the aircraft. The distribution of these loads must conservatively approximate or closely reflect the real situation. The structure must be able to withstand limited loads without harmful permanent deformation. Under any load up to the limit load, deformation shall not hinder safe operation. The structure must be able to withstand the ultimate load for at least three seconds without breaking, and the static test to the ultimate load must include the ultimate displacement and ultimate deformation caused by the load [13].

In terms of design and construction, the general rule is that the aircraft must not have design features or details that experience has shown to be dangerous or unreliable. Each questionable design detail and the suitability of the part must be determined through experiments. The applicability and durability of the materials used in the parts must meet the approved standards (such as industrial or military standards, or technical standards) to ensure that these materials have the strength and

other properties used in the design data. The design process considers the expected in service. Environmental conditions, such as temperature and humidity.

In terms of manufacturing methods, the manufacturing methods used must be able to produce a structure that is always intact. If a certain manufacturing process (such as gluing, riveting or heat treatment) needs to be strictly controlled to achieve this purpose, the process must be performed in accordance with the approved process specifications.

Since this article discusses the riveting process, the design requirements for fasteners are also introduced. Each detachable bolt, screw, nut, pin or other detachable fastener must have two sets of independent locking devices, because Its loss may prevent the continued flight and landing with normal driving skills and physical strength within the design limits of the aircraft. No self-locking nuts shall be used for any bolts undergoing rotation during use.

At the same time, each structural part must meet the requirements of the structural insurer, and be properly protected to prevent performance degradation or loss of strength due to weather, corrosion, abrasion and other reasons during use. Ventilation and drainage measures must be provided at the parts that must be protected.

4.2 The impact of aviation manufacturing on the environment

The general manufacturing industry is usually a resource-intensive industry. The environmental problems during the operation of various manufacturing activities include air pollutant discharge, water pollution, energy consumption, waste (solid and hazardous), and the environmental impact of the entire supply chain.

Air pollution, also known as air pollution, according to the definition of the International Organization for Standardization (ISO), air pollution usually refers to: due to human activities or natural processes causing certain substances to enter the atmosphere, showing a sufficient concentration, to reach a sufficient time, And therefore endanger the comfort, health and welfare of human beings or the

environment.[14]Air pollution may be generated locally, but it can spread over long distances, sometimes across continents through international weather patterns.

No one is immune from this kind of pollution. Air pollution comes from five main human activities. These pollution sources emit various substances, including carbon monoxide, carbon dioxide, nitrogen dioxide, nitrogen oxides, ground-level ozone, particulate matter, sulfur dioxide, hydrocarbons, and lead, all of which are harmful to human health [15]. The main activities of species are the burning of fossil fuels, wood and other biomass fuels indoors, industrial production, transportation, agricultural livestock and incineration and waste release. In the scope of this article, we mainly discuss the impact of aviation manufacturing and transportation on air pollution.

There are different classification methods for wastewater from different angles. According to different sources, it is divided into two categories: domestic wastewater and industrial wastewater; according to the chemical category of pollutants, it can be divided into inorganic wastewater and organic wastewater; there are also classified according to industrial sectors or production processes that produce wastewater, such as coking wastewater, metallurgical wastewater, and pharmaceuticals [16], waste water, food waste water, etc.

Freshwater pollution comes from many sources, including municipal, industrial and agricultural waste, waste water and nutrient loss, power generation, heavy industry, automobiles, etc. Around the world, about 2 billion tons of human waste are discarded in waterways every day. Severe organic pollution has affected about one-seventh of the rivers in Africa, Asia and Latin America, and has been steadily increasing over the years. This article mainly discusses industrial waste and water pollution from heavy industry.

Chemical pollution refers to the waste gas and pollutants produced during the production process of the chemical industry. Most of these wastes are harmful above a certain concentration, and some are highly toxic substances, which will cause pollution when entering the environment. Some chemical products will cause some

pollution during the use process, even more serious and more extensive than the pollution caused by the production itself.

The raw materials for aircraft manufacturing come from industrial production and mining. Major industrial accidents and long-term industrial mismanagement, especially in the extractive industry, can pollute large areas of land. Pollutants in the soil can be absorbed by crops and agricultural products, and have a direct and direct impact on human health.

According to «Environmental Trends in Aviation to 2050», international aviation emissions that affect the global climate and local air quality are expected to increase by approximately 2 to 4 times the 2015 level by 2050, depending on the type of emissions (CO₂, NO_x or PM) and the analysis scenario used .

The impact of aviation on the environment is because the heat, noise, particles and gases emitted by aircraft engines can cause climate change and global dimming. Aircraft emit particles and gases, such as carbon dioxide (CO₂), water vapor, hydrocarbons, carbon monoxide, nitrogen oxides, sulfur oxides, lead and black carbon, and interact with them and with the atmosphere. At the same time, the impact of aircraft maintenance and aircraft manufacturing on the environment cannot be ignored. The necessity and urgency of carbon reduction in the aviation industry are very prominent. With the increase in the number of aircraft, it is still a challenging task to continuously explore and improve various energy-saving and emission-reduction methods to achieve the established goal of carbon neutrality in the aviation industry.

Carbon peaking and carbon neutrality are gaining more and more cognition, consensus and active practice around the world. In many countries, relevant macro and industry policy formulations and technological innovations related to carbon reduction are underway. Entering 2021, the frequent occurrence of abnormal and extreme weather events in many places around the world has also made the residents of the global village more and more aware of the huge impact and destructive power that global warming can produce, making global carbon reduction activities more urgent.

Air transport is currently the fastest and most time-sensitive mode of transportation in human economic activities, and it has an irreplaceable empowering effect on China and international economic and trade development. The generation of carbon emissions during air transportation is highly related to the hardware structure and technology of the aircraft.

According to statistics from the International Energy Association (IEA), in the nearly 30 years before the outbreak of COVID-19, the global carbon dioxide emissions generated by the transportation industry have exceeded industrial carbon emissions, ranking second in the world. It is second only to the electric power and heating industry, which ranks first. If not controlled, 25% of the world's carbon emissions will probably come from the aviation industry by 2050.

The aircraft manufacturing industry will produce pollution, and its pollution sources mainly come from waste oil, waste emulsion, surface treatment sludge, waste tank liquid and other solid wastes, chromic acid mist, Waste gas such as hydrogen chloride, sulfuric acid mist, nitrogen oxides, VOCs, surface treatment wastewater containing COD_{Cr}, SS, petroleum and other pollutants, fluorescence detection wastewater, etc. These pollutants may be affected by wastewater discharge, gas deposition, solid waste stacking, etc. The surrounding soil is harmful and affects the current status of soil quality.

This paper optimizes the structure of aircraft riveted joints, which can reduce the impact of secondary bending on aircraft fatigue life during aircraft operations, effectively extend aircraft fatigue life, save materials and human resources for maintenance and repair, and can effectively reduce the environmental pollution of aviation industry process..

4.3 Methods how to protect the environment from this impact

In order to reduce the impact of aviation industry manufacturing on environmental pollution, countries around the world implement aviation sustainable development strategies. There are three major technical elements for the sustainable development of aviation industry:

1. Continue to develop aircraft and engine designs and technologies, and continue to pursue improvements in fuel efficiency and reduction of carbon dioxide emissions [17].

Aircraft and engine design and technology

In the past 40 years, the development of aircraft and engine technology has reduced carbon dioxide emissions per seat mile by more than 1% per year on average. This is the result of substantial R&D investment in materials, aerodynamic efficiency, digital design and manufacturing methods, turbomachinery development, and aircraft system optimization.

Over the years, through various industry organizations and international institutions, the aviation industry has consciously committed to achieving a series of positive goals for improving the environmental performance of aircraft. The target set by the European Aviation Research Advisory Committee requires that by 2050, compared with 2000, carbon dioxide emissions will be reduced by 75%, nitrogen oxide emissions will be reduced by 90%, and noise will be reduced by 65%.

To help achieve these positive goals, a global agreement can be reached through the International Civil Aviation Organization that requires fuel efficiency performance standards to be incorporated and applied to the certification process of each aircraft. Improve existing aircraft and engine designs, and continue to increase efficiency as much as possible.

2. Support the commercialization of sustainable alternative aviation fuels.

For the foreseeable future, aviation will continue to rely on liquid fuel as the basic energy source for large and long-range aircraft. Even under the most optimistic predictions of electric flight, the global regional and single-aisle commercial aircraft fleets will continue to operate on jet fuel in the coming decades. Therefore, the development of sustainable aviation fuel (SAF) that uses recycled raw materials instead of fossil carbon fuels and meets strong and reliable sustainability standards is an important part of a sustainable future.

3. Develop brand-new aircraft and propulsion technology to accelerate technological development that can realize the "third era" of aviation.

Building on the foundation laid by the Wright brothers and the innovators of the jet age in the 1950s, the aviation industry is ushering in its third important era. This era is achieved through advances in new structures, advanced engine thermodynamic efficiency, electric and hybrid propulsion, digitization, artificial intelligence, materials and manufacturing. Large aircraft will begin to benefit from new designs that will further improve efficiency by managing aircraft drag and allocating propulsion in new ways. The use of new materials will make the aircraft lighter, thereby further improving efficiency.

On the basis of the subject of structural optimization in this article, the structure is optimized to reduce the influence of unfavorable factors on the fatigue life of the aircraft. The unfavorable factors here refer to the phenomenon of secondary bending caused by structural factors.

The optimized riveting structure of the aircraft effectively reduces the influencing factors of secondary bending, extends the fatigue life of the aircraft to a certain extent, reduces the number of repairs and maintenance, saves material and labor costs, and indirectly reduces the industrial manufacturing process Pollution to the environment.

Conclusion to Part 4

The fourth part describes the safety requirements of aircraft construction for aircraft, introduces the impact of aviation manufacturing on the environment, and analyzes and discusses how to reduce the pollution of aviation manufacturing to the environment.

PART 5. LABOR PROTECTION

5.1 Introduction

This article proposes a structural optimization plan for the riveted parts of the aircraft. In order to verify the feasibility of the optimization plan proposed in this article, a control group modeling work and experimental verification are required. In order to provide the research and development results of the structural integrity of the aircraft, the process of experiment and modeling needs to use the analysis of the riveted structure of the aircraft and the analysis of stress and strain. The experimenter is an engineer who has experimental operation experience and is engaged in the processing of aviation materials. In this chapter, we will analyze and explain the working environment of the laboratory and the protective measures for the personal safety of laboratory personnel

5.2 Analysis of working conditions in the workplace

The laboratory is the main working place for scientific research personnel to conduct scientific research, and it is also the storage place for various valuable instruments. Once an accident occurs, it will cause property damage in the light of the cost of life. Laboratory safety management and safety awareness training are one of the important means to improve laboratory safety.

The laboratory safety system is composed of people, objects and the environment. People's safety awareness, safety responsibilities, safety knowledge; safe location and safety status of objects; environmental water, electricity, climate and accidents will all be decisive factors for experimental safety.

Laboratory safety work is a huge systematic project, which requires a complete organization, sound rules and regulations, strict safety education, supervision and management in place, and complete safety facilities.

5.2.1 Workplace organization

The laboratory will be designed to accommodate 2-3 people. Its area will be calculated as:

$$A = a \cdot b [m^2] \quad (5.1)$$

$$A = 15m \cdot 10m = 150m^2 \quad (5.2)$$

Where

A- area of the laborataty

a- length of the laboratory

b- width of the laboratory

Average working area per person is:

$$A_{person} = \frac{A}{n} [m^2] \quad (5.3)$$

$$A_{person} = \frac{150m^2}{3} = 50m^2 \quad (5.4)$$

Where

A_{person} - average working area per person

n-number of person

The space of the laboratory can be calculated as:

$$V = A \cdot h [m^3] \quad (5.5)$$

$$V = 150m^2 \cdot 3.5m = 525m^3 \quad (5.6)$$

Where

V- Laboratory volume

h- Laboratory height

All the parameters about the laboratory are designed according to the document:ДБН В.2.2-28:2010 " Administrative and domestic buildings" The laboratory needs to install 8 lights and 2 windows.

The most suitable microclimate working environment is:

Temperature:less than 24°C

Relative humidity: 50%

Air velocity: 0.2m/s

5.2.2 List of harmful and dangerous production factors

In the experimental operation process of this paper, the harmful production factors include physical factors:

- Microclimate: temperature, humidity, wind speed, heat radiation;
- Non-ionizing electromagnetic field and radiation: electrostatic field, constant magnetic field (including geomagnetic field), industrial frequency electric and magnetic field (50 Hz), electromagnetic radiation in the radio frequency range, electromagnetic radiation in the optical range (including laser and ultraviolet);
- Produce noise, ultrasonic, infrasound;
- Vibration (local, general);
- Lighting-natural (missing or insufficient), artificial (insufficient lighting, direct and reflected dazzling brilliance, pulsation of lighting).

5.2.3 Analysis of harmful and dangerous production factors

5.2.3.1 Microclimate in the work area

When the temperature, humidity, wind speed and heat radiation index exceed the maximum limit and do not meet the laboratory standards, harmful risks will occur, Temperature should be controlled less than 24°C, the relative humidity will not exceed 50%, and the air velocity will be around 0.2m/s.

5.2.3.2 Non-ionizing electromagnetic fields and radiation

In physics, radiation is considered to be a process in which energetic particles or waves propagate in space [18]. Because the energy of radiation itself is different, and the reaction mechanism of its interaction with matter is also different, we often divide radiation into two types: ionizing radiation and non-ionizing radiation. Generally, non-ionizing radiation is also called electromagnetic radiation. There will be electromagnetic radiation in the process operation during the riveting process, and improper operation will cause harmful hazards.

5.2.3.3 Produce noise, ultrasonic, infrasound

In the process of experimental operation and verification, the interaction between the machine and the structure will generate noise. If the range and magnitude of the noise are not well controlled, it will affect the health of the staff. Whether in production, life or entertainment, when a person is exposed to a noise environment, his health will be threatened. Short exposure time will cause anxiety and mental stress, which will distract attention; long exposure time will cause hearing loss or even deafness.

5.2.3.4 Static electricity

In the course of the experiment that needs to be done in this chapter, energized equipment is needed. Static electricity will be generated during the energized use process, which may indirectly cause harm.

Too strong static electricity is pathogenic. Static electricity in the body can cause abnormal conduction of brain nerve cell membrane currents, affecting the human central nervous system, resulting in changes in blood pH and body oxygen characteristics, making people feel fatigue, irritability, insomnia, and headaches. In severe cases, it may cause mental illness.

5.3 Labor protection measures

The basic task of labor protection is to continuously improve working conditions, make unsafe and health-harmful operations safe and harmless, mechanize and automate heavy manual labor, and achieve safe and civilized production. According to the factors that cause experimental harm, develop corresponding protective measures.

Control the laboratory temperature, humidity, wind speed, and heat radiation to meet the theoretical requirements, and monitor in time to prevent experimental hazards caused by the microclimate.

In order to prevent the influence of electromagnetic radiation, the following experimental arrangements are made: pay attention to the arrangement of electrical

appliances and do not place them in a centralized manner. Especially some electrical appliances that easily generate electromagnetic waves. Second, avoid operating electrical appliances for a long time and avoid multiple electrical appliances being activated at the same time. It is best to install a computer anti-radiation screen made of lead glass in the laboratory computer. Third, keep the distance between the human body and electrical appliances. The distance between fluorescent lamps should be 2-3 meters. When electrical appliances are not in use, it is best not to keep them in standby mode, because weak electromagnetic fields can be generated at this time, and radiation accumulation will also occur for a long time.

At present, riveting technology still occupies an extremely important position in the aircraft manufacturing process.[19] Because the connection strength of riveting is relatively stable and reliable, it is easy to check and troubleshoot, and it is suitable for more complicated structural connections. In particular, the connection between the skin and the frame in aerospace vehicles basically adopts the riveting process. At present, in the process of aircraft manufacturing, the production of aircraft fuselage, wings and tail section is still dominated by manual riveting. The riveting process used will generate high sound pressure level noise at the assembly site, which is specifically reflected in the rivet connection structure. In the process. According to the survey, the noise level of the riveting worker's work position reaches 124dB(A) (absolute decibel, the same below); the noise level measured at a distance of about 10 meters from the riveting work site is 102dB(A); it is still about 30 meters away. Achieved 92dB. These noise indicators far exceed the human body's ability to withstand noise, and have a great impact on human health.

The working environment adopts sound absorption, noise reduction and sound insulation measures, and the staff needs to wear protective equipment correctly-soundproof earplugs, protective earmuffs, soundproof helmets and helmets.

5.4 Fire safety at the production site

The room area for the experimental operation is 300 square meters and belongs to an industrial laboratory. The laboratory is used for the riveting work of aircraft

structure assembly. In this article, this laboratory is used to verify the significance and feasibility of the optimization effect of the riveting structure. The explosion and fire hazards in the workplace and the entire room are mainly caused by electrical appliances. Since the rivet contacts the rivets and components through the energized riveting machine, the electrical appliances will become the main cause of danger.

Due to the presence of live electrical appliances in the fire area, the type of fire is a live electrical equipment fire, and the fire extinguisher is a dry powder fire extinguisher or a carbon dioxide fire extinguisher.

Because the experiment involves the use of electrical appliances, improper operation or due to the influence of external conditions, and cause the impact of fire. The specific fire prevention measures are summarized as follows:

1. Strengthen safety education for students, learn safe self-rescue and escape methods. To
2. Regularly check the power lines on the test bench to eliminate fire hazards.
3. After the experiment is finished, let the lights rest. To
4. Strengthen the management of inflammable and explosive materials and implement the responsibility system. ...
5. When students are doing experiments, open the front and back doors of the laboratory and set up safe passages.
6. Flammable experimental waste should be properly handled to prevent fire.
7. Fire extinguishing materials such as wet towels and fire-resistant sand should be installed in the laboratory.
8. Keep the experimental materials hygienic and clean up flammable materials such as paper scraps and sundries in time.

Conclusion to Part 5

The fifth part introduces the workplace and working environment of the riveting experiment, arranges the organization of the workplace, enumerates the list of harmful and dangerous production factors, analyzes the harmful and dangerous

production factors, and analyzes the fire safety and labor of the production site The protection method is introduced.

GENERAL CONCLUSIONS

Riveting of aircraft components, skin to skin, skin to stringers, skin to frame, etc. is a main method for the aircraft structural joints. The components of the riveted joints belong to the category of Primary Structural Elements, i.e. elements responsible on the aircraft structural integrity. The riveted components of the primary structure withstand wide spectrum of loads exerted to the structure in flight and on the ground.

The service loads cause fatigue damage, which limits the service life of the aircraft.

The effect of the secondary bending, which is phenomena caused by the asymmetry of riveted lap joints exacerbates the fatigue problem.

To reduce the harmful effect of the secondary bending the presented work has been carried out. To gain the purpose of the secondary bending reduction the following problems where considered and solved.

Typical riveted joint for further stress-strain analysis have been defined.

The procedure of the finite element analysis for the selected component was defined.

Selected components have been analyzed by the FEM under the action of loads close to operational for the fuselage Principle Structural Elements.

Influence of the riveted joint geometry on the magnitude of the secondary bending has been analyzed.

Recommendation on the practical application of the Master work results have been developed and ready for use.

Labor protection problems were considered and recommendation have been developed.

Environmental protection problems were considered and measures to protect the environment were developed.

REFERENCES

1. Starikov R. Fatigue behavior of mechanically fastened aluminium joints tested in spectrum loading[J]. *International journal of fatigue*, 2004, 26(10): 1115-1127.
2. Johan Ekh. Joakim Schon, L. Secondary bending in multi fastener, composite-to aluminium single shear lap joints[J]. *Composite part B-Engineering*, 2005, 36(3): 195-208.
3. Skorupa M, Korbel A, Skorupa A, T. Machniewicz. Observations and analyses of secondary bending for riveted lap joints[J]. *International journal of fatigue*, 2015, 72: 1-10.
4. Schijve, J., Campoli, G., & Monaco, A. (2009). Fatigue of structures and secondary bending in structural elements. *International Journal of Fatigue*, 31(7), 1111-1123. (ARTICLES).
5. Joakim Schon, Johan Ekh. Effect of secondary bending on strength prediction of composite, single shear lap joints[J]. *Composites science and technology*, 2005, 65(6): 953-965.
6. Skorupa, M., Korbel, A., Skorupa, A., & Machniewicz, T. (2015). Observations and analyses of secondary bending for riveted lap joints. *International Journal of Fatigue*, 72, 1-10.
7. Skorupa, Małgorzata & Korbel, A. (2008). Modelling the secondary bending in riveted joints with eccentricities. *Arch Mech Eng*. 369-387.
8. Chaves, C.E., & Spinelli, H.D. (2003). ANALYSIS OF FASTENED JOINTS – PART 1: THE INFLUENCE OF SECONDARY BENDING.
9. Rijck, J & Fawaz, Scott. (2000). A Simplified Approach for Stress Analysis of Mechanically Fastened Joints. *Proceedings of the Fourth Joint Dod/FAA/NASA Conference on Aging Aircraft*.
10. Zhao, Libin & Xin, An & Liu, Fengrui & Zhang, Jianyu & Hu, Ning. (2016). Secondary bending effects in progressively damaged single-lap, single-bolt composite joints. *Results in Physics*. 6. 10.1016/j.rinp.2016.08.021.
11. De Rijck, J. J. M., Fawaz, S. A., Schijve, J., Benedictus, R., & Homan, J. J. (2007). Stress analyses of mechanically fastened joints in aircraft fuselages.

12. Machniewicz, T., Korbel, A., Skorupa, M., & Winter, J. (2018, November). Analytical, numerical and experimental investigation of the secondary bending of riveted lap joints. In AIP Conference Proceedings (Vol. 2028, No. 1, p. 020010). AIP Publishing LLC.
13. Smalley, C. L. Subject: AIRFRAME GUIDE FOR Date: 4/30/07 AC No: 23-19A CERTIFICATION OF PART 23 AIRPLANES.
14. ISO 4225:1994 (en) Air quality — General aspects — Vocabulary
15. Thurston, G. D. (2017). Outdoor air pollution: sources, atmospheric transport, and human health effects.
16. Yaseen, D. A., & Scholz, M. (2019). Textile dye wastewater characteristics and constituents of synthetic effluents: a critical review. *International journal of environmental science and technology*, 16(2), 1193-1226.
17. Lee, J., & Mo, J. (2011). Analysis of technological innovation and environmental performance improvement in aviation sector. *International journal of environmental research and public health*, 8(9), 3777-3795.
18. Leroy, C., & Rancoita, P. G. (2011). Principles of radiation interaction in matter and detection. World Scientific.
19. Wu, D. W., & Yuan, J. C. (2012). Based on flexible automation fixture of siding components of assembly craft planning and simulation. In *Applied Mechanics and Materials* (Vol. 224, pp. 109-112). Trans Tech Publications Ltd.